Journal of Medicinal Chemistry

pubs.acs.org/jmc

Perspective

Current Status and Perspectives of Novel Radiopharmaceuticals with Heterologous Dual-targeted Functions: 2013−2023

Zuojie Li, Qing Ruan, Yuhao Jiang, Qianna Wang, Guangxing Yin, Junhong Feng, and Junbo Zhang*

Cite This: J. Med. Chem. 2024, 67, 21644−21670

Read Online

ACCESS | Metrics & More | Article Recommendations

ABSTRACT: Radiotracers provide molecular- and cellular-level information in a noninvasive manner and have become important tools for precision medicine. In particular, the successful clinical application of radioligand therapeutic (RLT) has further strengthened the role of nuclear medicine in clinical treatment. The complicated microenvironment of the lesion has rendered traditional single-targeted radiopharmaceuticals incapable of fully meeting the requirements. The design and development of dual-targeted and multitargeted radiopharmaceuticals have rapidly emerged. In recent years, significant progress has been made in the development of heterologous dual-targeted radiopharmaceuticals. This perspective aims to provide a comprehensive overview of the recent progress in these heterologous dual-targeted radiopharmaceuticals, with a special focus on the design of ligand structures, pharmacological properties, and preclinical and clinical evaluation. Furthermore, future directions are discussed from this perspective.

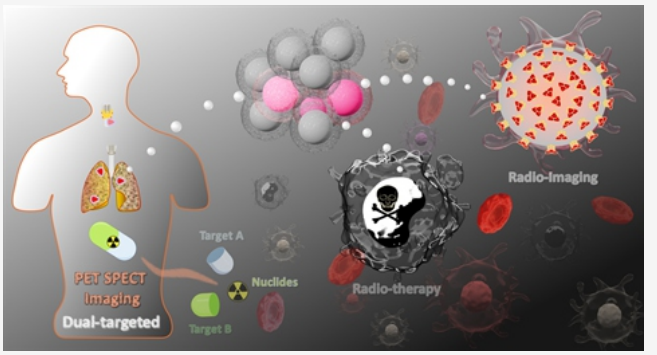

■ SIGNIFICANCE

Research on heterologous dual-targeted radiopharmaceuticals has become an important component of radiopharmaceutical development. This perspective explores recent applications and advances, systematically discusses the structural design, pharmacological properties, and preclinical and clinical evaluation of the most advanced heterologous dual-targeted radiopharmaceuticals. It highlights the advantages of the use of bioactive molecules obtained via this design strategy, and provides prospects for future strategies that may promote the development of heterologous dual-targeted radiopharmaceuticals.

1. INTRODUCTION

Molecular imaging has become a key component of pathological diagnosis and management and plays a significant role in oncology, cardiology, and neuroscience research.[1,2] Unlike structural and anatomical imaging, molecular imaging provides functional information by targeted tracers and their interactions with biological systems. In nuclear medicine, molecular tracers are drugs that carry radioactive isotopes and are commonly referred to as tracers.[3] From an imaging perspective, the field of nuclear medicine consists of two distinct but comparable imaging technologies: positron emission tomography (PET) and single-photon emission computed tomography (SPECT).[4−6] PET and SPECT provide molecular and cellular-level information in a noninvasive manner, making them important for detecting biochemical markers at early stages of disease development, often before clinical symptoms appear.[7,8]

Radiopharmaceuticals have important value in both diagnostic imaging and medication.[9] [^{18}F]Fludeoxyglucose ([^{18}F]FDG) has laid a foundation for research on radiopharmaceuticals and is known as the "century molecule" in the field of molecular imaging.[10] Although [^{18}F]FDG is the most widely used PET tracer in clinical practice, with the continuous growth of precision medicine demand, a series of more specific tracers that target specific biological targets have emerged. Especially in the past decade, with the continuous approval of the Food and Drug Administration (FDA), radiopharmaceuticals have rapidly been developed (Figure 1). For example, for neurodegenerative diseases, [^{18}F]Florbetapir, [^{18}F]Flutemetamol, and [^{18}F]-Florbetaben, which target Aβ (amyloid β-protein) in Alzheimer's disease, were approved between 2012 and 2014,[11] and [^{18}F]Fiortaucipir, which targets the tau protein, was approved for marketing in 2020.[12] In addition, [^{18}F]Fluorodopa for imaging Parkinson's syndrome was approved in 2019.[13]

Received: July 13, 2024
Revised: October 1, 2024
Accepted: November 26, 2024
Published: December 9, 2024

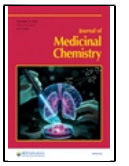

https://doi.org/10.1021/acs.jmedchem.4c01608
J. Med. Chem. 2024, 67, 21644−21670

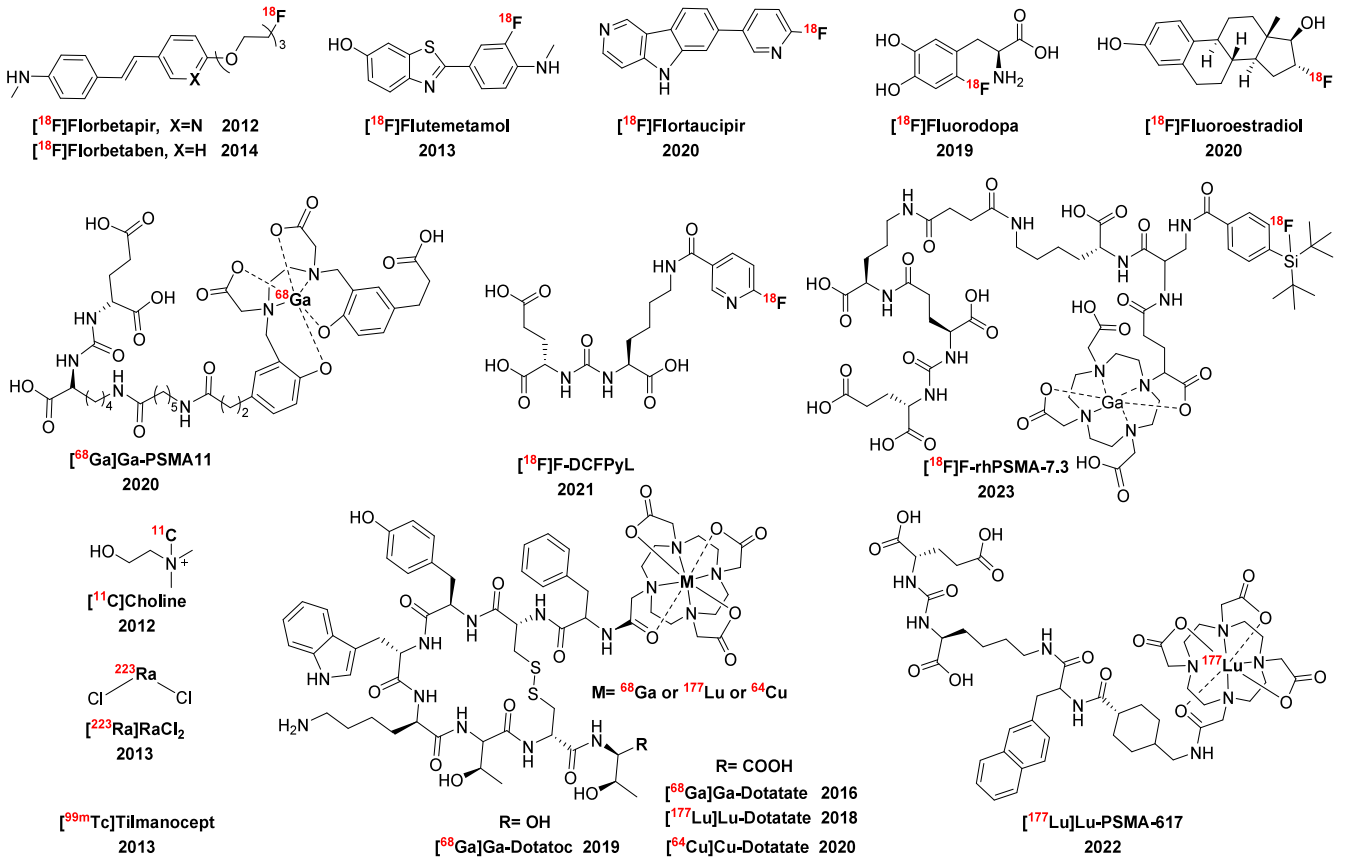

Figure 1. Radiopharmaceuticals approved by the FDA in the past decade.

These tracers provide powerful evidence for the early diagnosis of neurological system diseases. In oncology, the FDA approved [^{99m}Tc]Tilmanocept for localized diagnosis of lymph node metastasis in patients with breast cancer or melanoma in 2013,[14] and [^{18}F]Fluoroestradiol was approved in 2020 for imaging estrogen receptor-positive breast cancer.[15] [^{11}C]Choline was the first PET tracer approved by the FDA for prostate cancer detection,[16] followed by highly selective prostate-specific membrane antigen (PSMA)-targeted [^{68}Ga]Ga-PSMA11, [^{18}F]F-DCFPyL, and [^{18}F]F-rhPSMA-7.3 tracers that were subsequently approved between 2020 and 2023,[17,18] providing high accuracy for detecting PSMA-positive lesions in male cancer patients. In terms of RLT drugs, [^{223}Ra]$RaCl_2$ was approved by the FDA in 2013 for the treatment of advanced bone metastatic castration resistant prostate cancer.[19] [^{68}Ga/^{64}Cu/^{177}Lu]Ga/Cu/Lu-Dotatate was the first FDA approved integrated diagnostic and therapeutic drug for the diagnosis and treatment of gastrointestinal and pancreatic neuroendocrine tumors,[20] the derivative [^{68}Ga]Ga-Dotatoc exhibits the same diagnostic performance.[21] In 2022, [^{177}Lu]Lu-PSMA-617 was subsequently approved for PSMA-positive metastatic castration-resistant prostate cancer (mCRPC) patients, indicating that RLT has become a highly promising treatment option in clinical practice,[22−24] greatly stimulating enthusiasm for radiopharmaceutical research. In particular, the design and development of RLT drugs has further promoted new developments in radiopharmaceutical research.

Although the FDA has recently approved several radiopharmaceuticals for clinical diagnosis and treatment, there are still challenges in their subsequent clinical application.[25] For example, the sensitivity of the PSMA tracer is strongly affected by the concentration of prostate-specific antigen (PSA) in the patient's body, and there are issues with its high uptake values in the salivary glands.[26,27] [^{177}Lu]Lu-Dotatate has high abdominal uptake values in SPECT imaging, and there is a risk of radiation hazards (such as irreversible damage to the male reproductive system), including [^{177}Lu]Lu-PSMA-617.[28] Moreover, the complex heterogeneity of different types of tumors means that a single targeted tracer may not fully meet these requirements and that the expression levels of specific receptors may also change at different stages of the tumor.[29] These issues are constantly demanding stricter requirements for the design of radiopharmaceuticals: how to further improve tracer sensitivity and achieve specificity for disease targets while maintaining good pharmacokinetic properties, which is highly important for both radiation diagnosis and treatment, as well as the development of integrated diagnostic and therapeutic radiopharmaceuticals. Researchers are constantly optimizing their structures in an attempt to find new molecules with higher affinity and selectivity to obtain better performance, but issues such as lengthy cycles, high costs and low success rates have significantly complicated the development of new molecules. In general drugs development, the design of dual-target and multitarget drug molecules has become a commonly employed strategy owing to the success of combination drug therapy.[30,31] Oncology drugs (such as taretinib, ostinib, and azvudine) developed based on dual-targeted methods have shown significant advantages in overcoming drug off-targets and single-target resistance, improving drug activity and selectivity, reducing drug toxicity, improving bioavailability.[32,33] This will significantly reduce blindness in drug development and accelerate research and development progress. Therefore,

https://doi.org/10.1021/acs.jmedchem.4c01608
J. Med. Chem. 2024, 67, 21644−21670

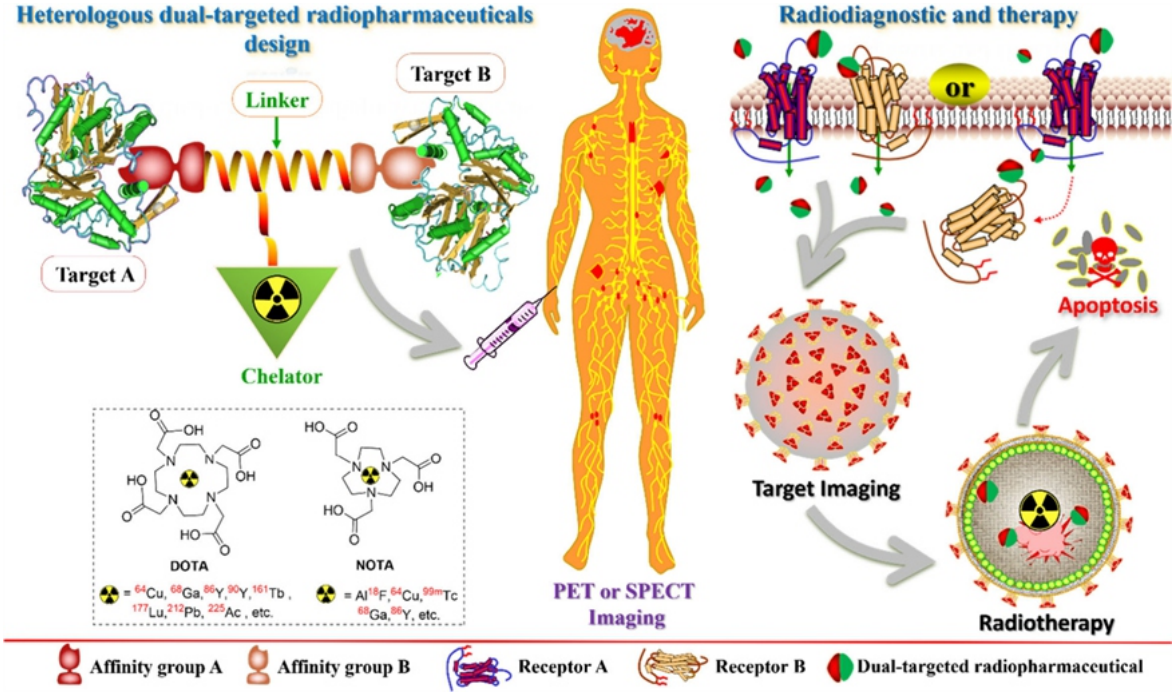

Figure 2. Dual-targeted radiopharmaceutical design strategy.

applying the concept of dual-target design to the study of radiopharmaceuticals is a feasible strategy. In recent years, new radiopharmaceuticals based on a dual-target design have been continuously investigated and have great potential for improving absolute target uptake, target-to-nontarget ratio, tolerability, treatment safety and the demonstrated clinical feasibility.

2. DUAL-TARGETED MOLECULAR DESIGN IN RADIOPHARMACEUTICALS

There are currently over 20,000 known targets in humans, and only approximately 600 of them have drugs for clinical or market use.[34] For radiopharmaceuticals, there are even fewer potential druggable targets. Radiopharmaceuticals, especially diagnostic drugs, were usually studied with highly differentially expressed proteins (such as PSMA, fibroblast-activating protein (FAP), trophoblast cell surface antigen-2 (Trop-2), etc.) and certain disease-specific biomarkers (such as Aβ, tau, etc.) as targets to improve the accuracy of tracers. The main research focus is on membrane proteins and transmembrane proteins, while relatively little research has been conducted on intracellular proteins (weakly targeted proteins may be the main factor for limiting their research), and the design of heterologous dual-targeted molecules may be a potential strategy to expand the research scope of radiopharmaceuticals. As shown in Figure 2, heterologous dual-targeted radiopharmaceuticals generally consist of three parts: affinity groups for two heterologous targets, linkers and chelators. Two of these heterologous targets can be both membrane proteins or a combination of membrane and intracellular proteins (heterologous dual-target effects are achieved through the high affinity groups of membrane protein entering the cell to bind intracellular targets), and the second functionalized group is highly important for improving the absolute uptake and accuracy of the target, as well as improving the molecular pharmacokinetic properties, especially in the development of radiopharmaceuticals for intracellular targets. In addition, the abundant linker fragments increase the molecular diversity and modification convenience. Finally, chelators, which are mainly composed of 1,4,7,10-tetraazacyclododecane-*N*,*N*′,*N*,*N*′-tetraacetic acid (DOTA) , 1,4,7-triazacyclononane-*N*,*N*′,*N*″-triaceticacid (NOTA), and their derivatives are used for the coordination of various radionuclides. Therefore, the design strategy of heterologous dual-targeted molecules is a reasonable way to further optimize performance and open a new perspective for radiopharmaceutical development and drug performance optimization.

3. NEW RADIOPHARMACEUTICAL WITH HETEROLOGOUS DUAL-TARGETED FUNCTION

In recent years, the number of studies on heterologous dual-targeted radiopharmaceuticals has increased significantly. These studies mainly focused on tumor-related targets, with PSMA and FAP as the main representatives. For the second target, researchers primarily select well-established albumin (ALB) and integrin for conjugation. Extensive research has been carried out on a series of heterologous dual-targeted radiopharmaceuticals through the incorporation of various radiolabels.

3.1. ALB Related Dual-targeted Radiopharmaceuticals. ALB is a single nonglycosylated peptide chain composed of 585 amino acids, with a molecular weight of 66.5 kDa. ALB is synthesized mainly in the liver and plays an important role in maintaining tumor pressure, maintaining plasma pH, and transporting and distributing various endogenous and exogenous ligands.[35] It is also the most abundant plasma protein, and owing to its long circulating half-life (approximately 19 d), it has become an important tool for improving the pharmacokinetic performance of drugs and an excellent drug delivery platform. Moreover, ALB accumulates in inflammatory and malignant tissues, which allows it to be applied as a specific target. 4-(4-Iodophenyl) butyric acid (IPBA) (**1**) and Evans blue (EB) (**2**) have good affinities for ALB and have been widely used in the design of radioactive dual-targeted drugs.[36−38]

https://doi.org/10.1021/acs.jmedchem.4c01608
J. Med. Chem. 2024, 67, 21644−21670

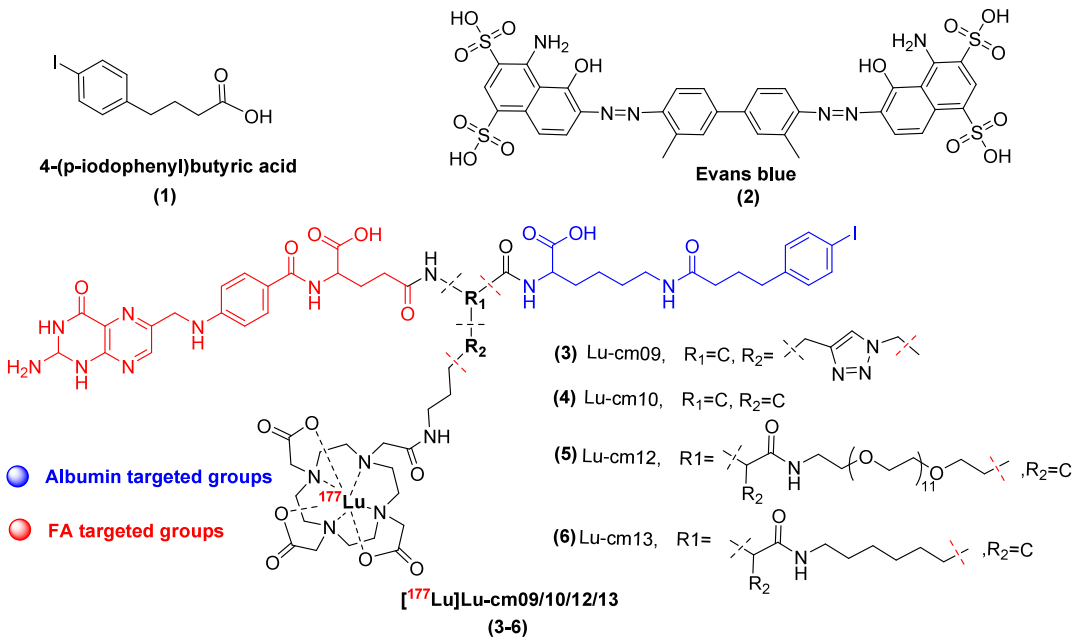

Figure 3. ALB targeted groups and ALB-FR dual-targeted radiopharmaceuticals.

3.1.1. ALB-FR Dual-targeted Radiopharmaceuticals. The folate receptor (FR) is highly expressed in various types of cancer with limited expression in normal tissues.[39] In recent years, FR-targeted strategies have shown promise in clinical research for anticancer effects and drug delivery, as well as preoperative and intraoperative imaging. However, owing to the high expression of FR in the proximal renal tubules,[40] the application of radiolabeled folate in RLT has not yet been achieved. Conjugation of ALB to FR targets in an attempt to prolong the circulation of radiolabeled folate and reduce its clearance and subsequent renal retention is a feasible strategy.

The ALB-FR dual-targeted radiopharmaceutical [^{177}Lu]Lu-cm09 (**3**)[41] was evaluated in a KB (FR+) mouse model (Figure 3). [^{177}Lu]Lu-cm09 showed highly tumor uptake (19.46% ID/g, 24 h), good retention in tumor tissue (6.72% ID/g, 5 d), significantly better than [^{177}Lu]Lu-EC0800 (without IPBA). Moreover, the renal radioactivity of [^{177}Lu]Lu-cm09 significantly decreased within 4 h, nearly three times better than [^{177}Lu]Lu-EC0800. One hour after injection, it reached a considerable background and gradually increased over time, with a tumor-to-blood ratio of 152 at 120 h. At 50 d after tumor treatment, a single dose of [^{177}Lu]Lu-cm09 (1 × 20 MBq) completely eliminated tumors in 4/5 mice and significantly improved mouse survival (>84 d vs blank group 27 d). Although there was no significant change in the weight of the mice during the treatment process, further studies have shown that they have a certain degree of nephrotoxicity. To further reduce their nephrotoxicity during treatment, optimizing the linker between the dual-targeted groups is an effective strategy. Three derivatives[42] ([^{177}Lu]Lu-cm10 (**4**), [^{177}Lu]Lu-cm12 (**5**), and [^{177}Lu]Lu-cm13 (**6**)) maintained good binding affinity to FR. Compared to [^{177}Lu]Lu-cm14 (without IPBA), the in vitro stability of the three radiotracers was improved, indicating that the introduction of ALB targeting groups has a positive impact on structural stability. SPECT imaging and biodistribution studies revealed that the tissue distribution properties of [^{177}Lu]Lu-cm10 and [^{177}Lu]Lu-cm13 linked by alkane chains were similar, with the tumor-to-kidney ratio being significantly better than that of [^{177}Lu]Lu-cm14. However, [^{177}Lu]Lu-cm12 linked by polyethylene glycol (PEG_{11}) leads to a decrease in tumor uptake and an increase in accumulation in the kidneys, resulting in a significant decrease in the tumor-to-kidney ratio. On the basis of the interaction between the three derivatives and serum proteins, alkane linking chains seem to have good tolerance and are more promising than introducing hydrophilic linking chains. Linker modification was not sufficient to improve renal uptake, but preinjection of pemetrexed (a folate metabolism antagonist) reduced renal uptake and doubled the tumor-to-kidney ratio. Therefore, the design strategy of folate-conjugated ALB is beneficial for prolonging the blood circulation time and increasing the tumor-to-kidney ratio, but notably, the design of radioactive folate ligands for treatment needs to balance renal toxicity and the risks of high-dose treatment.

3.1.2. ALB-SSTR Dual-targeted Radiopharmaceuticals. Somatostatin receptor (SSTR) is a G protein-conjugated receptor that regulates growth hormone secretion. SSTR2 is the most common and abundant subtype in tumor tissue and is especially prevalent in neuroendocrine tumors (NETs), where it plays an important role in signal transduction.[43] [^{177}Lu]Lu-Dotatate is the first approved radiotherapeutic drug for SSTR targets. Although it has been clinically applied, the overall effective rate (approximately 30%) is still relatively low, as in ^{177}Lu-labeled SSTR analogs, the kidney is the dose-limiting organ, followed by the bone marrow.[44] The ratio of the tumor dose to the renal dose can be defined as the treatment index (TI), with a higher TI being more favorable with rapid blood clearance and TI being the main reasons limiting its efficiency.[45]

[^{86}Y/^{90}Y]Y-DOTA-EB-TATE (**7**)[46] was prepared by conjugating an SSTR-targeted peptide with EB for SSTR2-targeted therapy. In the HCT116 (SSTR2+) mouse model, [^{86}Y]Y-DOTA-EB-TATE showed significant pharmacokinetic advantages compared with [^{86}Y]Y-DOTA-TATE (without EB), improving on the rapid clearance of [^{86}Y]Y-DOTA-TATE in the urinary tract with a maximum uptake in tumors (SSTR-tumors not taken up), resulting in better TBRs (tumor-to-

https://doi.org/10.1021/acs.jmedchem.4c01608
J. Med. Chem. 2024, 67, 21644−21670

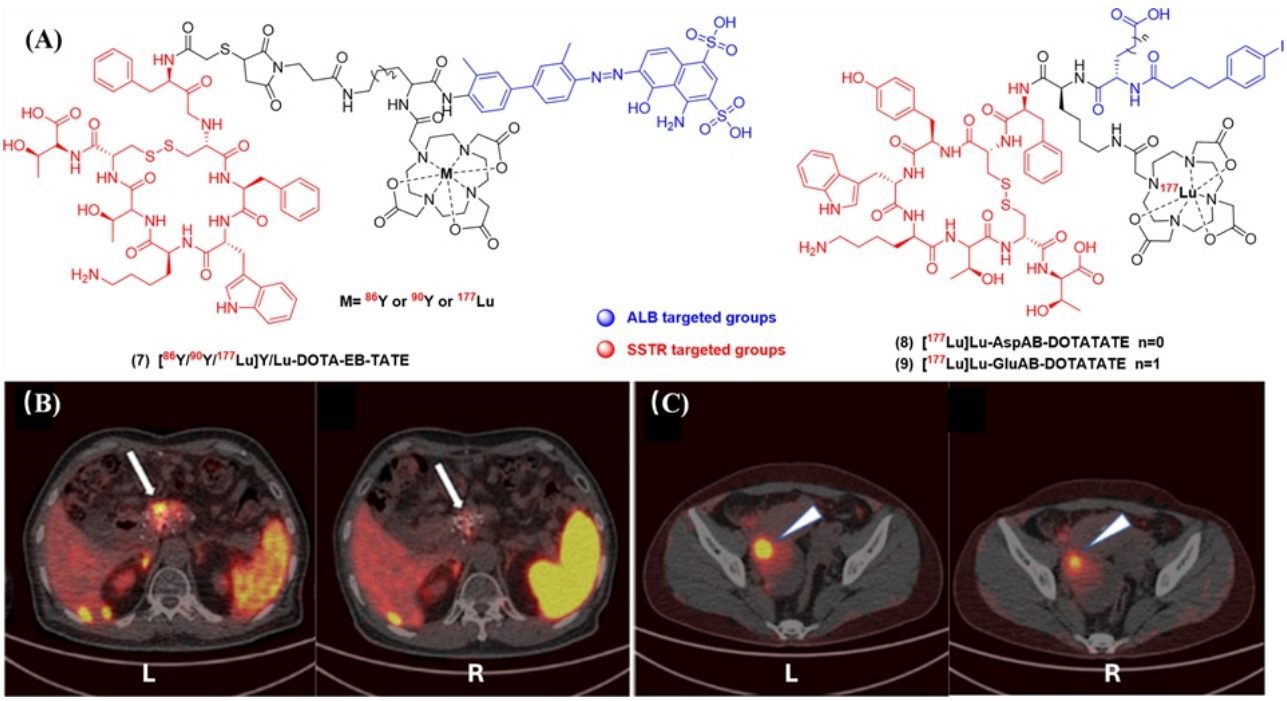

Figure 4. ALB-SSTR dual-targeted radiopharmaceuticals. (A) Structure of ALB-SSTR dual-targeted radiopharmaceuticals; (B) PET/CT images of a patient with NETs before (L) and 3 months after (R) single low-dose (19.5 mCi) [^{177}Lu]Lu-DOTA-EB-TATE treatment and (C) is single low-dose (105 mCi) of [^{177}Lu]Lu-Dotatate treatment before (L) and 1 months after (R). Figures B and C were reprinted with permission from ref 49. Copyright Ivyspring.

background ratios). The same trend was observed in the AR42J (SSTR2+) mouse model as in the HCT116 mouse model, which was coinjected with nonradioactive DOTA-EB-TATE, and the results revealed that the aggregation in the tumor was SSTR2 specific. [^{90}Y]Y-DOTA-EB-TATE showed significant antitumor activity in both mouse models constructed above, and the tumor completely disappeared at a dose of 1 × 7.4 MBq. Blood toxicity analysis revealed that it has good safety. The biodistribution of [^{177}Lu]Lu-DOTA-EB-TATE was greater than that of [^{177}Lu]Lu-Dotatate at all time points in the A427−7 (SSTR2+) mouse model. Notably, since the introduction of EB prolongs the circulation time of [^{177}Lu]Lu-DOTA-EB-TATE in the blood, its uptake in normal tissues is significantly greater than that of [^{177}Lu]Lu-Dotatate. In terms of treatment, a single dose of [^{177}Lu]Lu-DOTA-EB-TATE (1 × 18.5 MBq) completely regressed tumors in 4/5 mice. With the same antitumor activity, [^{177}Lu]Lu-DOTA-EB-TATE has a lower dose advantage than [^{177}Lu]Lu-Dotatate (3.7 MBq vs 18.5 MBq).[47] [^{177}Lu]Lu-DOTA-EB-TATE was further studied in 8 patients with advanced metastatic NETs.[48] No adverse symptoms were observed in the 5 patients who received a single dose (0.35−0.70 GBq) of [^{177}Lu]Lu-DOTA-EB-TATE, and the administration was well tolerated. In another group of 7 NET patients,[49] the use of approximately 1/6 the dose of [^{177}Lu]Lu-DOTA-EB-TATE had no difference in treatment effect with [^{177}Lu]Lu-Dotatate (Figure 4 B and 4 C) and was safety. Compared with [^{177}Lu]Lu-Dotatate, the SPECT imaging results revealed that [^{177}Lu]Lu-DOTA-EB-TATE had greater uptake and retention in NETs and significantly greater accumulation in the kidneys and bone marrow. In the treatment of 32 NET patients for up to 3 cycles,[50] three different doses (1.17−3.97 GBq/cycle) showed good tolerance and great potential for clinical application. It has now entered phase I clinical trials (NCT03308682).

In addition, [^{177}Lu]Lu-AspAB/GluAB-DOTA-TATE (**8**−**9**)[51] which uses IPBA as the ALB-targeted group, was compared with [^{177}Lu]Lu-Dotatate. Both had increased residence times in the blood and tumor uptake but a greater proportion of renal uptake, which reduced the TI and clinical practicality. Therefore, no antitumor activity studies have been conducted. For the above two types of ALB-SSTR heterologous dual-targeted radiopharmaceuticals, the ALB-targeted group EB seems to show better advantages than IPBA. Notably, the linker between the dual-targeted groups cannot be ignored.

3.1.3. ALB-PSMA Dual-targeted Radiopharmaceuticals. PSMA is a type II transmembrane protein composed of 750 amino acids. Its expression in prostate epithelial cells of prostate cancer patients is 100 to 1000 times greater than that in normal people. It is also expressed in the new blood vessels of solid tumors and is considered to be an ideal target for the diagnosis and treatment of prostate cancer.[27,52−54] In the past three years, based on the PSMA target, the FDA has approved a total of 3 diagnostic drugs and 1 therapeutic drug (Figure 1). It has become a hot target for radiopharmaceuticals and has also inspired researchers to explore new functions of PSMA. Glu-urea-Lys (EuK) oligopeptide molecules are highly selective for PSMA and are widely used in the study of PSMA targets. Owing to the pronounced charge properties of this specific targeted agent (facilitating polycarboxylate formation), rapid renal clearance emerges as a primary limiting factor for efficient drug delivery; however, these high charge characteristics are indispensable in maintaining a strong affinity toward PSMA. Therefore, bonding with ALB-targeted agents is a reasonable strategy to overcome this pharmacokinetic challenge. The dual-targeted design of ALB and PSMA has emerged as the most extensively researched area in current studies.

[^{131}I]I-RPS-001 (**10**)[55] is the first dual-targeted radiopharmaceutical with PSMA and ALB (Figure 5). The results

https://doi.org/10.1021/acs.jmedchem.4c01608
J. Med. Chem. 2024, 67, 21644−21670

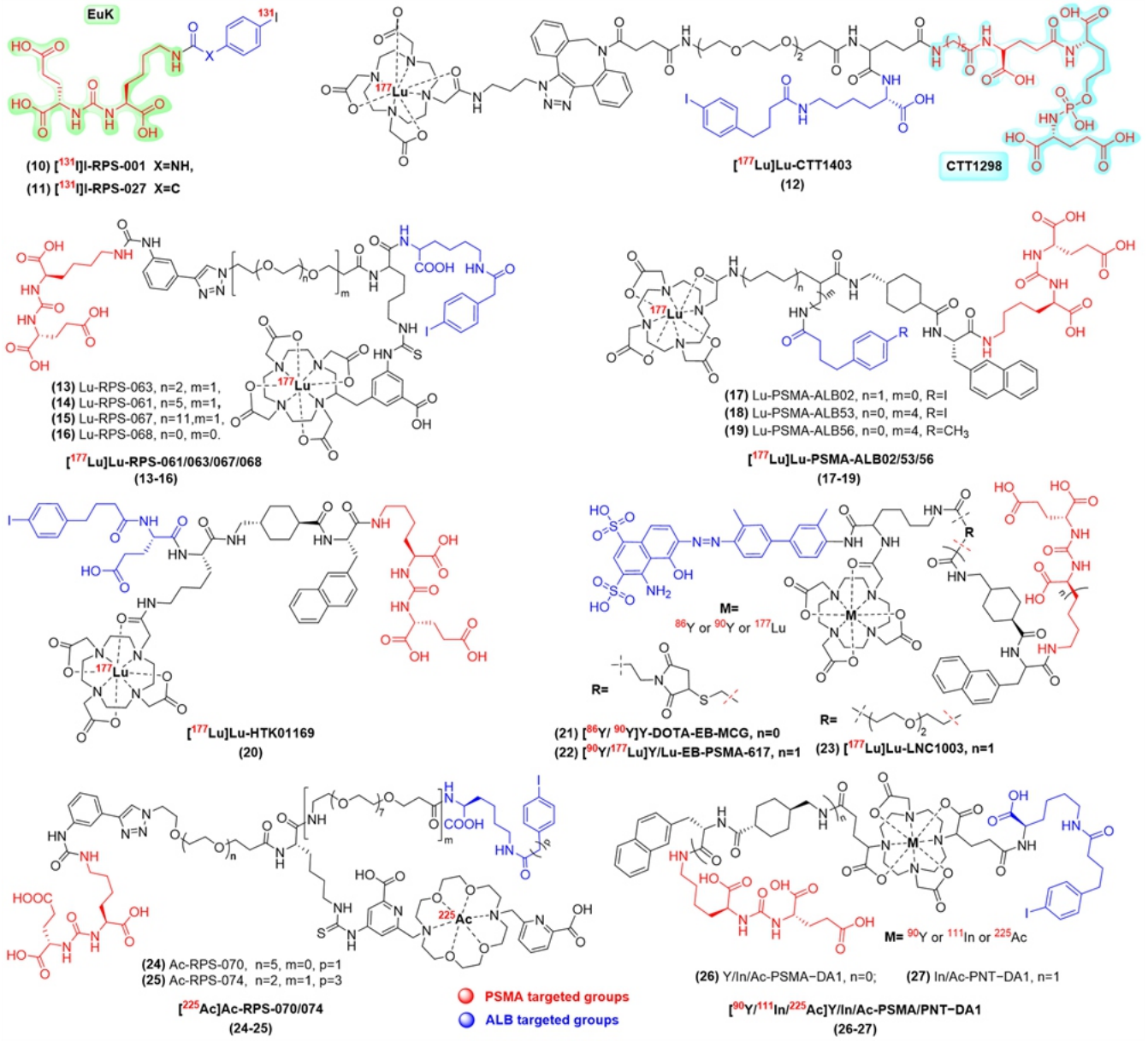

Figure 5. ALB-PSMA dual-targeted radiopharmaceuticals.

in 28 patients with advanced hormone-refractory and chemotherapy-refractory prostate cancer are encouraging. Preliminary efficacy was demonstrated by reductions in PSA, bone pain, and quality of life, as well as reductions in the size, extent, and number of lesions on diagnostic scans. Salivary and lacrimal glands are high-dose uptake organs, and a quarter of patients experience transient mild to moderate dry mouth. To date, the results of ^{124}I diagnostic and ^{131}I therapeutic administration have shown that it has good clinical application prospects. [^{131}I]I-RPS-027 (**11**)[56] is a derivative of [^{131}I]I-RPS-001 and has the most favorable biodistribution. In the LNCaP (PSMA++) mouse model, the maximum tumor uptake (12.41% ID/g) was reached 3 h after injection, and the tumor uptake was still as high as 8.13% ID/g at 24 h. The 24 h blood clearance rate was as high as 80%, and the clearance rate in other metabolic organs was basically consistent with the blood clearance rate. There were good TBRs 18 h after injection, and it showed higher specific tumor targeting as time progressed. Compared with that of [^{131}I]I-RPS-001 (without IPBA), although the tumor uptake of [^{131}I]I-RPS-027 was lower than that of [^{131}I]I-RPS-001 at all time points, the uptake in the kidney was 5 times lower than that of [^{131}I]I-RPS-001. This study demonstrated the effective binding of the ALB-targeted group IPBA to EuK. However, halogen-labeled radioactive therapeutic drugs have certain limitations in clinical applications.[52] A series of metal-coordinated PSMA and ALB heterologous dual-targeted radiopharmaceuticals have emerged.

[^{177}Lu]Lu-CTT1403 (**12**)[57] is a heterologous dual-targeted radioactive diagnostic and therapeutic integrated drug prepared by selecting a derivative of CTT1298 as a PSMA-targeted group and conjugating it with IPBA. The biodistribution in the PC3-PIP (PSMA+) mouse model revealed that [^{177}Lu]Lu-CTT1403 had greater tumor uptake than did [^{177}Lu]Lu-CTTP1401 (without IPBA) at all time points, and the maximum tumor uptake was 15-fold greater than that of [^{177}Lu]Lu-CTTP1401 (45.4 vs 3.00% ID/g), which effectively prolonged the retention

https://doi.org/10.1021/acs.jmedchem.4c01608
J. Med. Chem. 2024, 67, 21644−21670

of the drug in the tumor (24.2% ID/g, 168 h). Compared with [^{177}Lu]Lu-CTTP1401, [^{177}Lu]Lu-CTT1403 showed significant antitumor activity and had a significant advantage in prolonging the median survival of mice (>120 d vs 47 d), but the safety of the drug needs further evaluation.

[^{177}Lu]Lu-RPS-063 (**13**)[58] and its derivatives (**14**−**16**) were prepared using PEG of different lengths as linkers and DOTA as the metal chelator. In vitro enzyme activity inhibition experiments revealed that the length of the PEG polymer linker was inversely proportional to the PSMA affinity. The biodistribution in the LNCaP mouse model revealed that all of the radiotracers effectively internalized into the tumor, which was positively correlated with PSMA affinity. The maximum tumor uptake of [^{177}Lu]Lu-RPS-063 was significantly greater than that of [^{177}Lu]Lu-PSMA-617 (30.0 vs 14.40% ID/g, 4 h), and the uptake in nontarget organs was lower, resulting in better TBRs. Owing to its high and persistent tumor uptake advantage, the absorbed dose of [^{177}Lu]Lu-RPS-063 delivered to the tumor (96 h after injection) was 4 times greater than that of [^{177}Lu]Lu-PSMA-617, and the tissue distribution showed good pharmacokinetic characteristics. RLT deserves further investigation. Interestingly, the presence or absence of PEG chains has a significant impact on the kinetics. Compared to [^{177}Lu]Lu-RPS-063/61/07, [^{177}Lu]Lu-RPS-068 (without PEG chains) (**16**) has a difference in the time to reach the maximum tumor uptake (4 h vs 24 h). At the same time, the length of the PEG chain is positively correlated with the clearance rate of the tracer in the kidney and blood, showing that the introduction of PEG chains to reduce uptake in nontarget organs (especially the kidneys) is an effective strategy, but the effect is also on the maximum uptake and retention rate in the tumor can be seen. The balance between the two deserves attention in further radiotracers research.

Since its approval, [^{177}Lu]Lu-PSMA-617 has attracted widespread attention from researchers.[22] It is reasonable to introduce ALB-targeted groups into the [^{177}Lu]Lu-PSMA-617 molecular system to rectify its insufficient tumor delivery. First, the effects of linkers of different lengths (D-aspartic acid) on the pharmacokinetics and tissue distribution of IPBA derivatives were studied. [^{177}Lu]Lu-PSMA-ALB-02 (**17**)[59] became the best candidate, but it did not show obvious advantages over [^{177}Lu]Lu-PSMA-617. SPECT imaging of the PC3-PIP mouse model revealed that the tumor-to-blood ratio (176 vs 2730) and tumor-to-kidney ratio (7.16 vs 49.5) of [^{177}Lu]Lu-PSMA-ALB-02 were significantly lower than those of [^{177}Lu]Lu-PSMA-617. For the two derivatives [^{177}Lu]Lu-PSMA-ALB-53 (**18**) and [^{177}Lu]Lu-PSMA-ALB-56 (**19**), more lipophilic alkane chains were chosen as linkers.[60,61] The retention of [^{177}Lu]Lu-PSMA-ALB-53 in the blood was significantly better than that of [^{177}Lu]Lu-PSMA-ALB-56, resulting in differences in the time to reach the maximum tumor uptake (75.7% ID/g, 96 h vs 104% ID/g, 24 h). Both showed good tumor uptake, but [^{177}Lu]Lu-PSMA-ALB-56 had lower uptake in other nontarget organs and was cleared faster, resulting in better tumor-blood and tumor-kidney ratios. Notably, in the comparison between the two derivatives, the substitution of only one halogen group in the IPBA group had a significant effect on the pharmacokinetics, which provides a special perspective for the local optimization of drug performance. Owing to its favorable tissue distribution characteristics, [^{177}Lu]Lu-PSMA-ALB-56 was studied for its antitumor activity. With the same single dose (1 × 5.0 MBq), [^{177}Lu]Lu-PSMA-ALB-56 completely eliminated the tumors in 4/6 mice, which was significantly better than [^{177}Lu]Lu-PSMA-617 and it also showed great potential in prolonging the median survival of mice (>84 d vs 32 d). SPECT/CT imaging in 10 mCRPC patients revealed that [^{177}Lu]Lu-PSMA-ALB-56 was well tolerated, and no serious adverse events were observed. The mean uptake in the tumor was 2.3 times greater than that of [^{177}Lu]Lu-PSMA-617. Notably, uptake in the salivary glands also showed the same upward trend. Therefore, PSMA dual-targeted [^{177}Lu]Lu-PSMA-ALB-56 shows great diagnostic and therapeutic potential, especially in tumor treatment, and deserves further clinical research.

On the basis of the same design concept, [^{177}Lu]Lu-HTK01169 (**20**)[62] had a relatively high affinity for PSMA (K_i = 0.04 nM). Its biodistribution in the LNCaP mouse model revealed that the maximum tumor uptake of [^{177}Lu]Lu-HTK01169 was significantly greater than that of [^{177}Lu]Lu-PSMA-617 (55.9 vs 15.1% ID/g) and that [^{177}Lu]Lu-HTK01169 had a good antitumor effect because of its slower clearance rate in the blood (56.4% ID/g, 120 h). In the RLT study, [^{177}Lu]Lu-HTK01169 only required 1/4 of the dosage to achieve the same therapeutic effect as [^{177}Lu]Lu-PSMA-617. The same dosage (1 × 18.5 MBq) could significantly prolong the median survival of mice (>120 d vs 58 d). However, its pharmacokinetic properties and safety of administration deserve further study.

[^{86}Y/^{90}Y]Y-DOTA-EB-MCG (**21**)[63] is another (EB is an ALB-targeted group) ALB-PSMA dual-targeted radiopharmaceutical. [^{86}Y]Y-DOTA-EB-MCG had greater tumor uptake (40.40 vs 17.1% ID/g) than [^{86}Y]Y-DOTA-MCG (without EB) and had a better antitumor effect in the PC3-PIP mouse model. Tumor growth in the [^{90}Y]Y-DOTA-EB-MCG (1 × 7.4 MBq) treatment group was significantly reduced, and no obvious toxicity was observed in any of the treated mice. The DOTA-EB-MCG radioligand was reasonably effective for dual-targeting with conjugated EB and EuK. On this basis, EB-conjugated [^{90}Y/^{177}Lu]Y/Lu-EB-PSMA-617 (**22**)[64,65] was designed and synthesized. PET/CT imaging revealed that the maximum uptake of [^{90}Y]Y-EB-PSMA-617 in tumors was increased by approximately 4-fold and 2-fold compared with that of [^{86}Y]Y-PSMA-617 and [^{86}Y]Y-IPBA-PSMA-617 (IPBA is an ALB-targeted group), respectively. Its high and persistent accumulation in tumors results in high radiotherapeutic activity. A single dose (1.85 MBq) of [^{90}Y/^{177}Lu]Y/Lu-EB-PSMA-617 can completely regress a tumor, and pathological and hematological toxicity analyses revealed good safety. At the same dosage, its antitumor activity is significantly better than that of [^{90}Y/^{177}Lu]Y/Lu-PSMA-617 and [^{90}Y/^{177}Lu]Y/Lu-IPBA-PSMA-617. For this study, the ALB-targeted group EB seems to have more potential for improving pharmacokinetics than does IPBA. Recent studies have shown that the clinically negative therapeutic indicators of [^{177}Lu]Lu-PSMA-617 may be related to low PSMA expression levels.[66] [^{177}Lu]Lu-LNC1003 (**23**)[67] was shown to have better performance through further optimization of the linker, and pharmacokinetic and antitumor activity studies were conducted in a 22Rv1 (PSMA+) mouse model. The tumor uptake of [^{177}Lu]Lu-LNC1003 was significantly greater than that of [^{177}Lu]Lu-EB-PSMA-617 and [^{177}Lu]Lu-PSMA-617 (138.87 vs 29.89 vs 4.28% ID/g), and the low uptake by nontargeted organs resulted in high-contrast SPECT/CT images 24 h after injection. For the modification strategies of the two linkers, when the targeted groups are the same, the linker modified with PEG seems to have more advantages than the heterocycle does, and the improvement in pharmacokinetics is obvious. A single dose (18.5 MBq)

https://doi.org/10.1021/acs.jmedchem.4c01608
J. Med. Chem. 2024, 67, 21644−21670

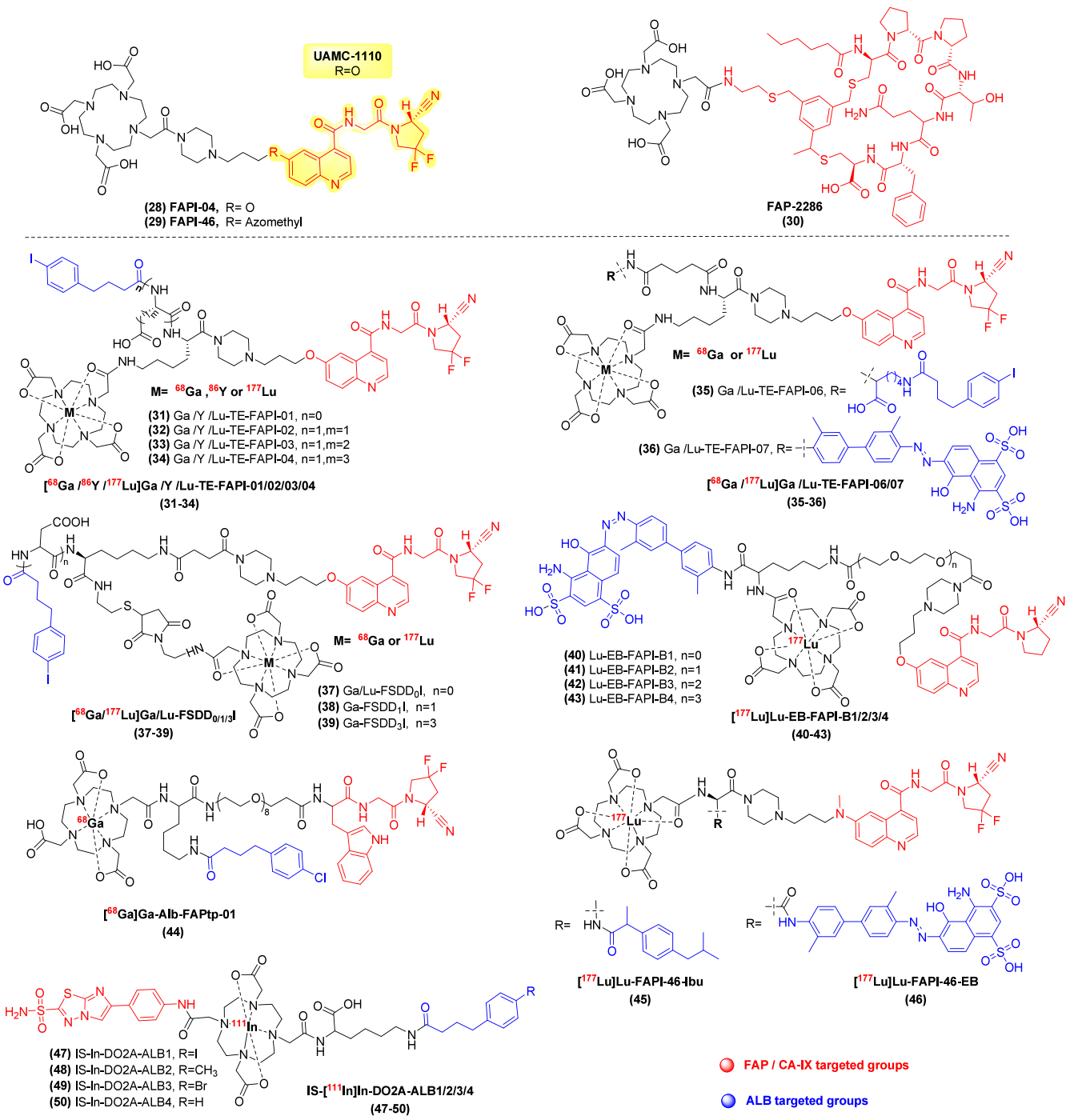

Figure 6. ALB-FAP and ALB-CA-IX dual-targeted radiopharmaceuticals.

significantly inhibited the growth of 22Rv1 tumors, whereas [^{177}Lu]Lu-PSMA-617 was almost ineffective under the same conditions. [^{177}Lu] Lu-LNC1003 shows significant advantages in the treatment of prostate cancer, especially in prostate lesions with moderate PSMA expression levels, is expected to become a new generation of radiopharmaceuticals for the treatment of different PSMA expression levels, and it has been approved for clinical trials.

[^{225}Ac]Ac-PSMA-617 has shown satisfactory results in the treatment of mCRPC patients, especially in patients who have failed to respond to [^{177}Lu]Lu-PSMA-617, showing incomparable advantages, which has greatly promoted the research of α-radiotherapeutic nuclides.[68,69] [^{225}Ac]Ac-RPS-070 (**24**)[70] is the first radiopharmaceutical for ALB-PSMA dual-targeted radioligand α-nuclide therapy, thereby offering valuable insights to advance the clinical development of radiotherapeutic nuclides. In the LNCaP mouse model, [^{225}Ac]Ac-RPS-070 had good uptake and slow clearance rates in tumors. Uptake in other nontarget organs was negligible at 96 h after injection, and mouse tumors gradually regressed during treatment. The pharmacokinetic performance of [^{225}Ac]Ac-RPS-074 (**25**)[71] was further improved, and the tumor uptake was still as high as 11.90% ID/g at 14 d after injection. In a study of antitumor activity, it showed a dose-dependent effect. After a single dose (148 kBq) for 75 d, PET imaging and dissection confirmed that the tumors of 6/7 mouse completely regressed, with good long-

https://doi.org/10.1021/acs.jmedchem.4c01608
J. Med. Chem. 2024, 67, 21644−21670

term tumor inhibition activity and drug safety. [^{225}Ac]Ac-RPS-074 shows great potential for treatment and clinical translation. ^{90}Y/^{111}In/^{225}Ac-PSMA-DA1 (**26**)[72] is an ALB-PSMA heterologous dual-targeted diagnostic and therapeutic integrated radiopharmaceutical prepared with IPBA as the ALB targeted group. The tumor uptake and retention of [^{111}In]In-PSMA-DA1 were significantly greater than those of [^{111}In]In-PSMA−DB (without IPBA), and better TBRs was observed, allowing the acquisition of clear SPECT/CT images. In the LNCaP mouse model, [^{111}In]In-PSMA-DA1 resulted in lower renal uptake than did [^{111}In]In-PSMA-617, and the tumor-to-kidney ratio improved to a certain extent. Although the [^{225}Ac]Ac-PSMA-DA1 treatment group (1 × 20 kBq) had a significant inhibitory effect on tumor growth, the weight and survival rate of the 6 mice in the group were not affected during the treatment period, and it did not show an advantage over [^{225}Ac]Ac-PSMA-617. Unfortunately, [^{90}Y]Y-PSMA-DA1 (1 × 3.7 MBq) had poor activity and obvious toxicity during the treatment process. Notably, the performance differences after the coordination of different radioactive metals to the same chelating agent are obvious, which may be related to the properties of the nuclide itself (such as decay mode, energy size, radiation range, etc.)[73] and the coordination mode of the nuclide. By changing the length of the linker, [^{111}In/^{225}Ac]In/Ac-PNT-DA1 (**27**)[74] with better affinity was optimized, and its biological distribution and SPECT/CT imaging results were better than those of [^{111}In]In PSMA-DA1. [^{225}Ac]Ac-PNT-DA1 has stronger antitumor activity than [^{225}Ac]Ac-PSMA-617 does, and the radiation dose accumulated in the tumor is approximately 7.4 times greater than that of [^{225}Ac]Ac-PSMA-617. Satisfactorily, it is able to inhibit tumor growth at the lowest dose (1 × 2.5 kBq), although high-dose (5 or 10 kBq) treatment is safe based on blood and tissue analysis. In addition, compared with [^{225}Ac]Ac-RPS-074 and [^{225}Ac]Ac-PSMA-617,[71] [^{225}Ac]Ac-PNT-DA1 shows a significant low-dose advantage. Moreover, it has a relatively high tumor-to-kidney ratio (1.74 vs 0.49), showing great potential in overcoming the common nephrotoxicity of [^{225}Ac]Ac-PSMA-617 in clinical practice and has great clinical application value.

3.1.4. ALB-FAP Dual-targeted Radiopharmaceuticals. FAP is a membrane-bound type II serine protease belonging to the proline-specific protease S9 family. It is overexpressed in tumor-associated fibroblasts but is essentially not expressed in normal tissues. It plays an important role in tumor growth and metastasis.[75] Owing to its high specificity, it has become an ideal target for tumor diagnosis and treatment. The discovery of UAMC-1110 (a highly selective FAP inhibitor) opened up the study of FAP in radiopharmaceuticals,[76] and the development of radioactive diagnostic and therapeutic drugs targeting FAP has become a hot area of research.[77] FAPI-based radiotracers (such as FAPI-04 (**28**), FAPI-46 (**29**), and FAP-2286 (**30**), etc.; Figure 6) have shown initial advantages in clinical diagnosis, but their rapid clearance from blood and tumors limits their application in RLT.[78] Therefore, introducing ALB-targeted groups into the FAPI system is a feasible strategy to further optimize their pharmacokinetic performance.

[^{68}Ga/^{86}Y/^{177}Lu]Ga/Y/Lu-TE-FAPI-n derivatives (**31**−**34**)[79] are ALB-FAP heterologous dual-targeted radiopharmaceuticals conjugated with IPBA and FAPI-04, and their pharmacokinetic properties were evaluated in an HT-1080-FAP (FAP+) mouse model. [^{68}Ga]Ga-TE-FAPI-04 (**34**) showed the most favorable biodistribution. Compared with that of [^{68}Ga]Ga-FAPI-04, the circulation half-life of [^{68}Ga]Ga-TE-FAPI-04 in the blood was significantly greater (26.8 min vs 52.7 min). Tumor uptake and clear TBRs could be achieved within the half-life of ^{68}Ga ($t_{1/2}$ = 68 min), and a moderate circulation period was suitable for ^{86}Y for subsequent diagnosis. The tumor accumulation of [^{177}Lu]Lu-TE-FAPI-04 was ten times greater than that of [^{177}Lu]Lu-FAPI-04 (3.86 ID/g vs 0.34 ID/g) at 24 h after injection, and the uptake in normal tissues was low. In the Ga-TE-FAPI-01−04 series structure, the selection of linkers clearly has a crucial effect on the pharmacokinetics. Moreover, different ALB-targeted groups also present different metabolic properties. Compared with [^{68}Ga/^{86}Y]Ga/Y-FAPI-04, [^{68}Ga/^{86}Y]Ga/Y-TE-FAPI-06 (IPBA as the ALB targeted group) (**35**), and [^{68}Ga/^{86}Y]Ga/Y-TE-FAPI-07 (EB as the ALB targeted group) (**36**)[80] showed significant improvements in tumor uptake and retention, and the differential uptake and radioactive blockade in HT-1080-FAP and HT-1080 (FAP-) mice demonstrated the high specificity of the tracer for FAP. Further in vivo metabolic evaluation in pancreatic cancer model mice revealed that [^{177}Lu]Lu-TE-FAPI-06 and [^{177}Lu]Lu-TA-FAPI-07 still had high tumor uptake 96 h after injection, and the clearance rate of [^{177}Lu]Lu-TA-FAPI-07 in nontarget organs was greater than that of [^{177}Lu]Lu-TA-FAPI-06. Undoubtedly, the introduction of the ALB group has a clear advantage in increasing tumor uptake, and in terms of clearance to nontarget organs, EB seems to be potentially superior to IPBA. RLT studies revealed that the antitumor activity of [^{177}Lu]Lu-TA-FAPI-06&07 was significantly better than that of [^{177}Lu]Lu-FAPI-04 at the same dosage (3.7 MBq), but the tumor inhibition levels were comparable and dose dependent. Preliminary toxicity analysis proved that it had good safety. Therefore, compared with the radioligand FAPI-04, ALB-targeted TA-FAPI-06&07 has certain advantages in tumor diagnosis and treatment applications, but the absolute uptake value in the tumor and the target-to-nontarget ratio still have considerable potential for optimization, which deserves further study.

ALB-FAP heterologous dual-targeted tracers [^{68}Ga]Ga-FSDD$_n$I derivatives (**37**−**39**)[81] was shown to be effective in a mouse model of hepatocellular carcinoma derived from a human patient. Compared with [^{68}Ga]Ga-FSDD$_1$I (**38**) and [^{68}Ga]Ga-FSDD$_3$I (**39**), [^{68}Ga]Ga-FSDD$_0$I (**37**) had the longest blood circulation cycle and greater tumor uptake and retention. The carbon chain elongation under this modification strategy seems to be negative, and the Log *D* (a parameter for measuring the coefficient of lipid water distribution) of the three tracers is positively correlated with the in vivo performance, which means that the effect of lipid−water pairs on pharmacokinetics may be of great concern. [^{177}Lu]Lu-FSDD$_0$I had clearer SPECT/CT tumor images than did [^{177}Lu]Lu-FAPI-04, and the tumor could be clearly identified at 1 h after injection. The maximum tumor uptake was reached at 8 h, and it was effectively cleared in nontarget organs. The TBRs were still visible at 96 h. Among the three derivatives, FSDD$_0$I presented the most favorable pharmacokinetic characteristics, and its application in RLT needs further study.

Radiolabeled FAP-02 related tracers play an important role in the diagnosis of FAP-related diseases.[82] [^{177}Lu]Lu-EB-FAPI-Bn (**40**−**43**)[83] derivatives use the ligands FAP-02 and EB as targeted groups for FAP and ALB, respectively. SPECT images revealed that, with the exception of [^{177}Lu]Lu-EB-FAPI-B1 (**40**), the other three derivatives presented high and persistent uptake in the kidney, making them unsuitable for use as RLT drugs. Similarly, the length of the PEG chains was negatively

https://doi.org/10.1021/acs.jmedchem.4c01608
J. Med. Chem. 2024, 67, 21644−21670

correlated with aggregation in nontarget organs. In the U87MG (FAP+) mouse model, [^{177}Lu]Lu-EB-FAPI-B1 reached maximum tumor uptake 24 h after injection and had a good antitumor effect. High-contrast SPECT images of the low uptake of the tracer in nontarget organs were obtained, and the radioactive blocking experiment proved that the tracer showed FAP-specific uptake in the tumor. RLT studies have shown that [^{177}Lu]Lu-EB-FAPI-B1 can effectively inhibit tumor growth at three different doses (7.4 MBq, 18.5 MBq and 30 MBq) and has good safety. Recent clinical research[84] has shown that [^{177}Lu]Lu-EB-FAPI-B1 ([^{177}Lu]Lu-LNC1004) has a significant therapeutic effect after two doses (2 × 3.33 GBq) in mRAIR-TC (metastatic radioiodine-refractory thyroid cancer) patients, with the advantage of high radiation dose delivery to tumor lesions, and it is well tolerated. It has entered phase I clinical trials (NCT05723640).

[^{68}Ga]Ga-Alb-FAPtp-01 (**44**)[85] was produced by modifying the structures of the classical ligands UAMC-1110 and IPBA to investigate the potential application of dual-targeted tracers in tumor staging and prognostic assessment. [^{68}Ga]Ga-Alb-FAPtp-01 requires a 10-fold higher concentration of FAPI-04 to block uptake in U87MG cells, resulting in a stronger affinity for FAP. This modification of the structure of the targeted group is bold and innovative, enriching and expanding the diversity of molecular structures. PET images revealed that the maximum tumor uptake of [^{68}Ga]Ga-Alb-FAPtp-01 was comparable to that of [^{68}Ga]Ga-FAPI-04, but the clearance rate in the liver and kidney was significantly greater than that of [^{68}Ga]Ga-FAPI-04. Owing to the lower background uptake, the tumor-to-muscle ratio increased (5.9−9.5) over time, so the obtained PET/CT images presented greater contrast. Tumor growth was accompanied by changes in the expression level of FAP,[85] and the radioactivity of [^{68}Ga]Ga-Alb-FAPtp-01 in U87MG tumors was positively correlated with the volume of the tumor, indicating the potential application of tracer imaging in tumor staging. As a supplement to existing tracers, it has important clinical research value, especially in the prognostic assessment of various tumor types.

Based on the FAPI-46 structure design, [^{177}Lu]Lu-FAPI-46-Ibu (**45**) and [^{177}Lu]Lu-FAPI-46-EB (**46**) were compared head-to-head with [^{177}Lu]Lu-FAPI-46 (small molecule), [^{177}Lu]Lu-FAPI-46-F1D (small molecule dimer), and [^{177}Lu]Lu-FAP-2286 (cyclic peptide), providing a more intuitive analysis of the differences in FAP tracer design strategies between heterodimers and monomers, homodimers or cyclic peptides.[86] Compared with [^{177}Lu]Lu-FAPI-46, [^{177}Lu]Lu-FAPI-46-Ibu and [^{177}Lu]Lu-FAPI-46-EB exhibit comparable or even enhanced affinity for the FAP protein. Biodistribution indicates that in the HT-1080-hFAP model (with low FAP expression), [^{177}Lu]Lu-FAPI-46-F1D exhibits the maximum tumor uptake, followed by [^{177}Lu]Lu-FAPI-46, [^{177}Lu]Lu-FAPI-46-Ibu, [^{177}Lu]Lu-FAPI-46-EB and [^{177}Lu]Lu-FAP-2286 (10.47 vs 9.63 vs 8.40 vs 5.02 vs 3.42% I.A./g, 4 h). In the HEK-293-hFAP model (with high FAP expression), the maximum tumor uptake were as follows: [^{177}Lu]Lu-FAP-2286 > [^{177}Lu]Lu-FAPI-46-F1D > [^{177}Lu]Lu-FAPI-46-EB > [^{177}Lu]Lu-FAPI-46> [^{177}Lu]Lu-FAPI-46-Ibu (22.99 vs 17.16 vs 12.58 vs 10.34 vs 5.03% I.A./g, 4 h). Interestingly, the same tracer type exhibits significant differences in different mouse models, suggesting that the impact of model differences needs to be taken into account when evaluating radiotracers. In both models, [^{177}Lu]Lu-FAPI-46-EB showed the highest tumor retention rates (83% and 54%, respectively). The introduction of the EB significantly improves tumor retention, yet the selection of the ALB targeting agent is critical to the performance of ALB heterologous dual-targeted tracers. For this study, homodimeric and cyclic peptide tracers are superior to ALB-FAP heterodimers in increasing absolute tumor uptake and TBRs. However, the implications of the deficiencies in the molecular structural design of heterodimeric tracers cannot be overlooked. It should be recognized that homodimers, heterodimers, or cyclic peptides are potential strategies to improve the performance of small molecule monomer tracers.

3.1.5. ALB-CA-IX Dual-targeted Radiopharmaceuticals. CA-IX (carbonic anhydrase 9) is located on the cell surface and is not expressed in normal tissues except for the gastrointestinal tract.[87] It plays an important role in tumor invasion and metastasis; therefore, it is considered a promising target for cancer diagnostic imaging. Many CA-IX imaging tracers based on antibodies or small-molecule CA-IX inhibitors have been reported in recent years, but most tracers show significant renal accumulation and low tumor uptake, limiting further applications in clinical practice.[88,89]

IS-[^{111}In]In-DO2A-ALBn (**47**−**50**)[90] derivatives are dual-targeted tracers for ALB-CA-IX. Their pharmacokinetic properties vary according to the substituent groups of the IPBA moiety, with IS-[^{111}In]In-DO2A-ALB4 (**50**) showing the strongest ALB affinity in vitro but the worst in vivo imaging. These findings indicate that target affinity and pharmacokinetic performance are not completely unified and that pharmacokinetic performance is determined by multiple factors. IS-[^{111}In]In-DO2A-ALB1 (**47**) showed the most favorable imaging potential, with a significantly improved tumor-to-kidney ratio compared with that of [^{111}In]In-DO3A-IS1 (without IPBA) in the HT-29 (CA-IX+) mouse model, and clear SPECT images were obtained. Therefore, the ALB-targeted group significantly improved the pharmacological properties of CA-IX ligands, confirming the effectiveness and rationality of the combination of ALB and CA-IX targets, which is worthy of further in-depth study.

In summary, compared with single targeted homologues, ALB dual-targeted radiopharmaceuticals have shown satisfactory effects in prolonging the drug circulation half-life, improving disease target dose delivery, and improving pharmacokinetic properties. Therefore, using ALB as the second target is a reasonable and effective design strategy, and it is also the most promising combination in the development of dual-targeted radiopharmaceuticals. The delicate balance between ALB and other targets provides a reference and guidance for the subsequent development of ALB dual-targeted radiopharmaceuticals.

3.2. Integrin Related Dual-targeted Radiopharmaceuticals. Integrin is a heterodimeric transmembrane glycoprotein. Subtype $\alpha_v\beta_3$ is highly expressed in activated endothelial cells, newly formed blood vessels and some tumor cells. It has been widely studied in radiopharmaceuticals because of its obvious tissue expression differences.[91] Arg-Gly-Asp (RGD) is a short peptide with high affinity and selectivity for the integrin $\alpha_v\beta_3$. RGD cyclic peptide tracers show good uptake in tumors, but their rapid blood clearance and nonspecific uptake limit their further development.[92] Owing to its good affinity, the RGD group has been widely studied in dual-target and multitarget drug design and has shown good druggability.[93] Therefore, this method provides a new idea for research on the combined design of integrins and other targets as new radioactive diagnostic and therapeutic drugs.

https://doi.org/10.1021/acs.jmedchem.4c01608
J. Med. Chem. 2024, 67, 21644−21670

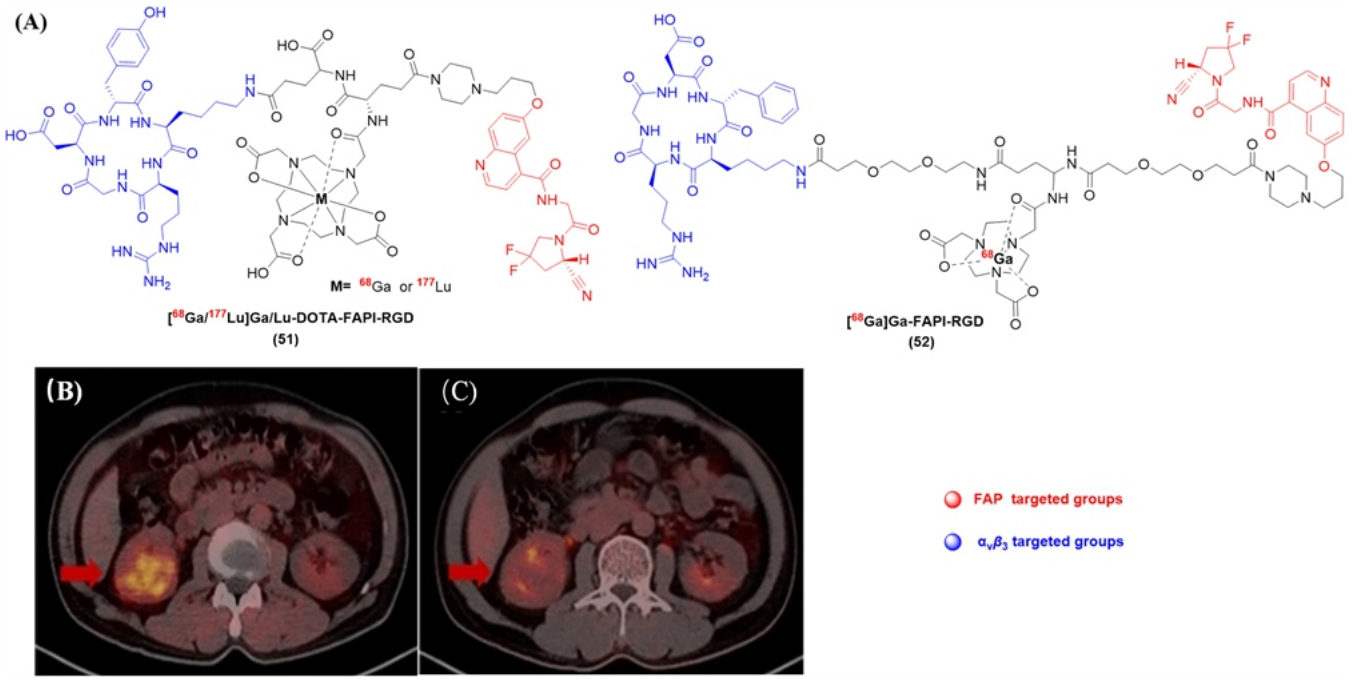

Figure 7. $\alpha_v\beta_3$-FAP dual-targeted radiopharmaceuticals. (A) Structure of $\alpha_v\beta_3$-FAP dual-targeted radiopharmaceuticals; (B) [^{68}Ga]Ga-FAPI-RGD PET/CT images of renal cell carcinomat and (C) is [^{18}F]FDG. Figures B and C were reprinted with permission from ref 95. Copyright the Authors.

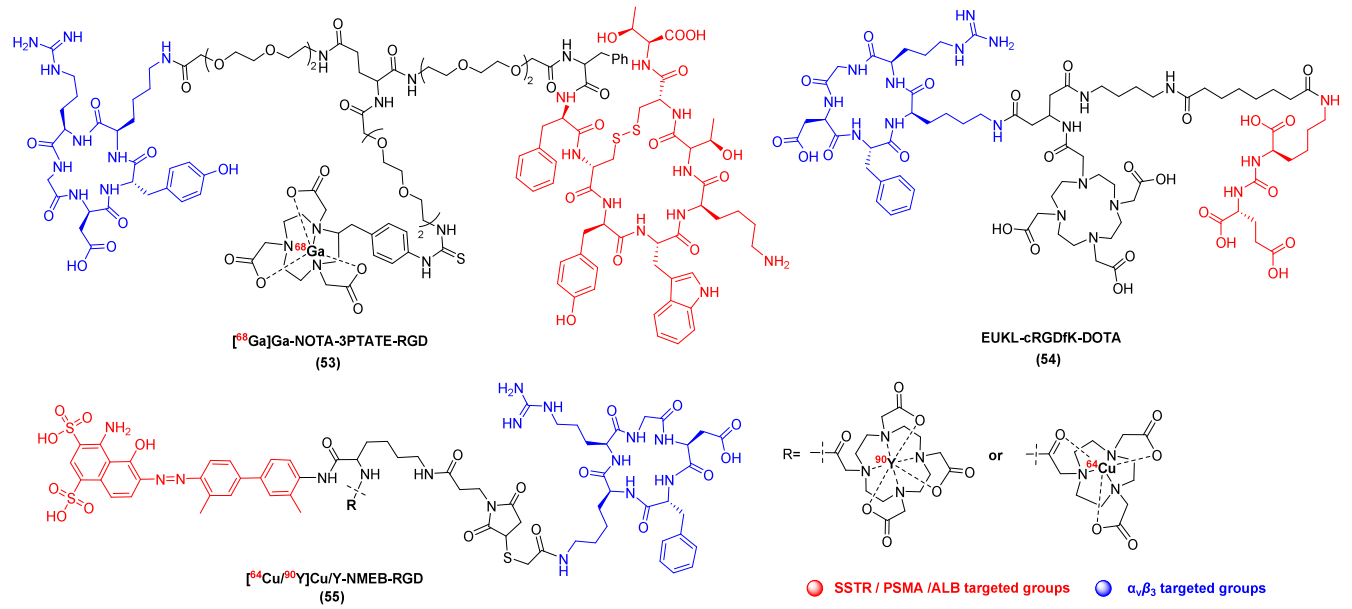

Figure 8. $\alpha_v\beta_3$-SSTR2, $\alpha_v\beta_3$-PSMA, and $\alpha_v\beta_3$-ALB dual-targeted radiopharmaceuticals.

3.2.1. $\alpha_v\beta_3$-FAP Dual-targeted Radiopharmaceuticals. Although great progress has been made in the development of integrin $\alpha_v\beta_3$- and FAP-selective targeted agents for imaging and therapy, their clinical application is still limited owing to the heterogeneous and multifactorial nature of tumors.[78] Therefore, heterodimeric or multimeric specific agents have emerged as new and exciting precise diagnostic and effective therapeutic strategies that overcome the limitations of current radiopharmaceuticals.

Radioactive nuclide ^{68}Ga-labeled $\alpha_v\beta_3$-FAP heterodimer DOTA-FAPI-RGD (**51**)[94] had good affinity for both FAP and integrin $\alpha_v\beta_3$. [^{68}Ga]Ga-DOTA-FAPI-RGD showed high specific uptake in U87MG (FAP+, $\alpha_v\beta_3$+) cells, and its PET images and biodistribution in a U87MG mouse model were superior to those of its corresponding monomeric radioligands. The tumor uptake of [^{177}Lu]Lu-DOTA-FAPI-RGD peaked at 4 h (22.1%ID/g) and was still well retained within 168 h (4.1% ID/g). DOTA-FAPI-RGD not only has good imaging applications but also may be used in cancer treatment via therapeutic nuclide-labeled heterodimeric ligands.

The $\alpha_v\beta_3$-FAP dual-targeted tracer [^{68}Ga]Ga-FAPI-RGD (**52**)[95] significantly improved tumor uptake, tumor retention time, tumor-targeted efficiency, and pharmacokinetic performance. As shown in Figure 7B and 7C, the first human distribution study revealed that [^{68}Ga]Ga-FAPI-RGD significantly improved tumor uptake (SUV_{max} = 5.1 vs 2.7) compared with [^{18}F]FDG in

https://doi.org/10.1021/acs.jmedchem.4c01608
J. Med. Chem. 2024, 67, 21644−21670

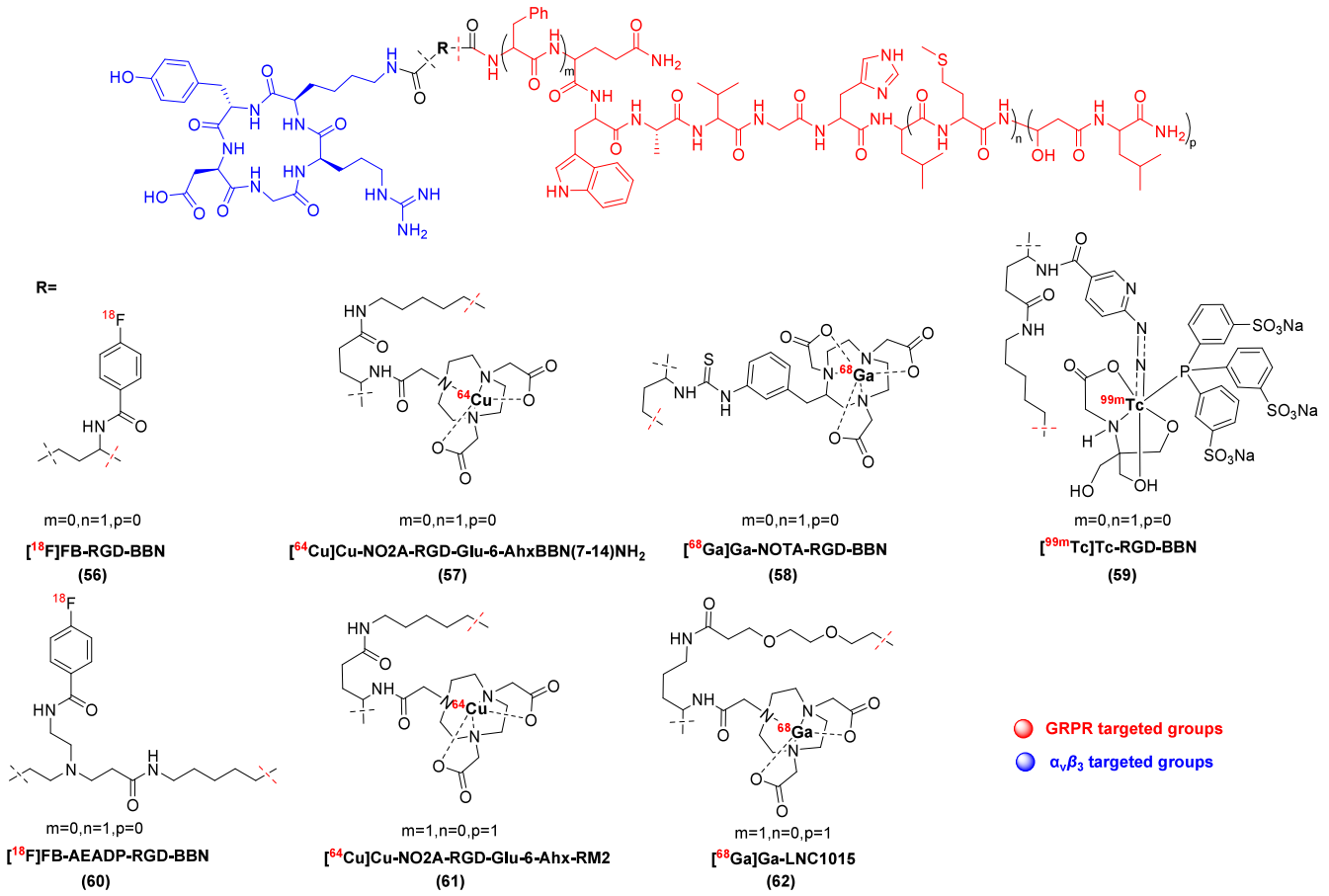

Figure 9. $\alpha_v\beta_3$-GRPR dual-targeted radiopharmaceuticals.

patients with renal cancer, and the TBRs increased over time, indicating high diagnostic performance and good tracer kinetics for potential therapeutic applications. It has good clinical application value and deserves further study.

3.2.2. $\alpha_v\beta_3$-SSTR2 Dual-targeted Radiopharmaceuticals. [^{68}Ga]Ga-3PTATE-RGD (**53**)[96] is a novel $\alpha_v\beta_3$-SSTR2 dual-targeted heterodimer tracer that exhibits good pharmacokinetic properties and high target-to-nontarget ratios in H69 and A549 mouse models (Figure 8). Compared with monomeric TATE and RGD peptides, [^{68}Ga]Ga-3PTATE-RGD showed better and broader tumor targeting ability, which justified its further study in detecting SSTR2- and integrin $\alpha_v\beta_3$-related cancers; however, it has not yet undergone radiation therapy research.

3.2.3. $\alpha_v\beta_3$-PSMA Dual-targeted Radiopharmaceuticals. EUKL-cRGDfK-DOTA (**54**),[97] a product of heterologous dual-targeted design for PSMA and $\alpha_v\beta_3$, has not yet been radiolabeled. The EUKL-cRGDfK-IRDye800 (DOTA just replaced by IRDye800) coupled with IRDye800 (fluorescent group) showed good specificity for both PSMA and integrin $\alpha_v\beta_3$, and fluorescence imaging showed good aggregation within the tumor. Research into fluorescent tracers has laid a theoretical foundation for the development of PSMA and $\alpha_v\beta_3$ dual-targeted radiopharmaceuticals. Once the metal chelator DOTA took the place of IRDye800, the wide variety of nuclides will significantly expand the application areas of PSMA-$\alpha_v\beta_3$ heterodimer tracers. It is worth looking at the application of the radioligand EUKL-cRGDfK-DOTA, which carries various nuclides, in the future diagnosis and treatment of diseases.

3.2.4. $\alpha_v\beta_3$-ALB Dual-targeted Radiopharmaceuticals. Owing to the affinity of EB for ALB, the construction of heterodimeric dual-targeted radiopharmaceuticals by $\alpha_v\beta_3$ and ALB is a reasonable strategy to address the limitations of single-targeting with $\alpha_v\beta_3$. PET images revealed that in the U87MG ($\alpha_v\beta_3$+) mouse model, [^{64}Cu]Cu-NMEB-RGD (**55**)[98] had greater tumor uptake than any single targeted homologue at all time points. The maximum tumor uptake of [^{64}Cu]Cu-NMEB-RGD was more than 10 times greater than that of [^{64}Cu]Cu-RGD (without EB), while the radioactivity in the blood was significantly reduced after 4 h, and a high-contrast PET image was obtained at 24 h. During 30 d of tumor treatment, [^{90}Y]Y-NMEB-RGD exhibited dose-dependent antitumor activity in the U87MG mouse model, with two administrations (2 × 7.4 MBq) leading to complete tumor regression and prolonged survival (>30 d, blank group for 13 d), whereas [^{90}Y]Y-RGD (without EB) did not show effective antitumor activity. Therefore, radioactive EB-RGD drugs based on a dual-targeted design have obvious advantages in both imaging and therapy are worthy of further clinical research.

3.2.5. $\alpha_v\beta_3$-GRPR Dual-targeted Radiopharmaceuticals. Gastrin-releasing peptide receptor (GRPR) is overexpressed in mainly androgen-dependent human prostate tissue, thus providing a potential target for the diagnosis and treatment of prostate cancer.[99] Bombesin (BBN), which was originally isolated from frog skin, is an analog of gastrin-releasing peptide. BBN can specifically bind to GRPR and is metabolically stable when applied in vivo.[100] Several BBN peptides have been labeled with various radioisotopes for the diagnosis and treatment of

https://doi.org/10.1021/acs.jmedchem.4c01608
J. Med. Chem. 2024, 67, 21644−21670

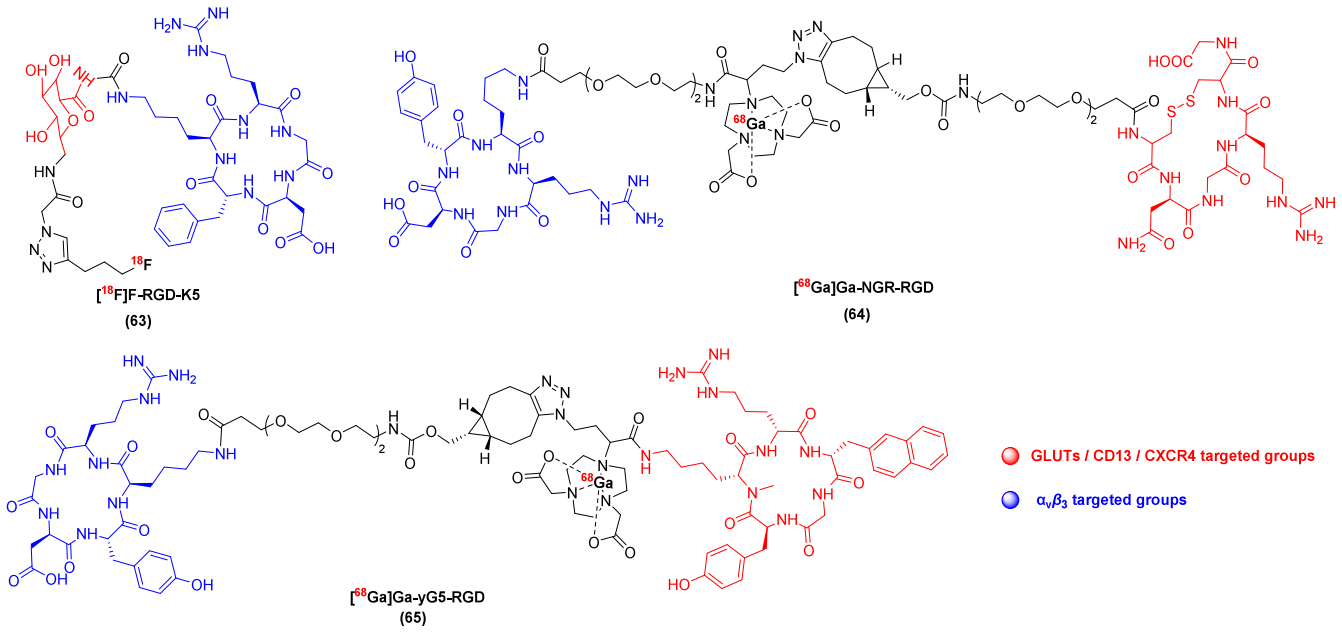

Figure 10. $\alpha_v\beta_3$-GLUTs, $\alpha_v\beta_3$-CD13, and $\alpha_v\beta_3$-CXCR4 dual-targeted radiopharmaceuticals.

GRPR-positive prostate lesions. However, radiolabeled monomeric BBN tracers have relatively low tumor accumulation and retention as well as unfavorable hepatobiliary excretion.[101] Therefore, to obtain better tumor-targeting effects and imaging quality, before 2013, Chen, Wang, Smith, and others[101−105] studied the conjugation of BBN and RGD and obtained [^{18}F]FB-RGD-BBN (**56**), [^{64}Cu]Cu-NO2A-RGD-Glu-6-AhxBBN(7−14)NH_2 (**57**), [^{68}Ga]Ga-NOTA-RGD-BBN (**58**), and [^{99m}Tc]Tc-RGD-BBN (**59**), research on their relevant pharmacological properties has been conducted mainly in the preclinical stage (Figure 9).

[^{18}F]FB-AEADP-BBN-RGD (**60**)[106] was not further studied because of its poor affinity for the target, which means that the selection of a suitable linker is an important step in the development of heterologous dual-targeted radiopharmaceuticals. The $\alpha_v\beta_3$-GRPR heterologous dual-targeted tracer [^{64}Cu]Cu-NO2A-RGD-Glu-6-Ahx-RM2 (**61**)[107] was optimized from the structure of NO2A-RGD-Glu-6-AhxBBN (7−14) NH_2, which has good affinity for both GRPR and $\alpha_v\beta_3$. In the PC3 mouse model, [^{64}Cu]Cu-NO2A-RGD-Glu-6-Ahx-RM2 exhibited rapid tumor uptake and a tumor stasis effect (4.26% ID/g, 24 h), which can produce clear PET images 4 h after injection. The good pharmacokinetic properties and sustained tumor uptake of [^{64}Cu]Cu-NOTARGD-Glu-6Ahx-RM2 are worthy of further study for imaging of $\alpha_v\beta_3$- and GRPR-positive tumors and possible radiotherapy.

[^{68}Ga]Ga-NOTA-RGD-BBN (**58**)[108] has entered clinical research in recent years. In 13 patients diagnosed with prostate cancer by biopsy, the safety and effectiveness of [^{68}Ga]Ga-NOTA-RGD-BBN in the diagnosis and staging of prostate cancer were demonstrated. In 22 female breast cancer patients, both primary cancer and metastatic lesions were positive for [^{68}Ga]Ga-NOTA-RGD-BBN accumulation. Clinical data[109] have shown that $\alpha_v\beta_3$ and GRPR dual-targeted [^{68}Ga]Ga-NOTA-RGD-BBN PET/CT is highly valuable for distinguishing primary prostate cancer, breast cancer, axillary lymph node metastasis and distant metastasis and has great potential for clinical application.

The $\alpha_v\beta_3$-GRPR heterodimer radiotracer [^{68}Ga]Ga-LNC1015 (**62**)[110] was prepared by changing the linker. The tracer demonstrated good binding affinity and specificity in vitro and in vivo. At all time points examined, tumor uptake, retention and TBRs were significantly improved by [^{68}Ga]Ga-LNC1015 compared with a single targeted homologue during PET imaging of the PC3 mouse model. In a preliminary clinical study of 11 patients with breast cancer, the tumor uptake and TBRs of primary and metastatic lesions of [^{68}Ga]Ga-LNC1015 PET/CT were significantly greater than those of [^{18}F]FDG and were more effective in identifying primary tumor sites and metastases. It has great potential to provide more precise information in the process of tumor diagnosis and stage, may be used to monitor metastasis during treatment, and has great potential for clinical application.

3.2.6. $\alpha_v\beta_3$-GLUTs Dual-targeted Radiopharmaceuticals. Glycoconjugated metal complexes may find useful applications in cancer, as they enter cells via glucose transporters (GLUTs) membrane proteins.[111] Radionuclide-labeled modified glucose derivatives, among which [^{18}F]FDG is the most widely used tracer in clinical practice, have good application value in disease diagnosis.[112] In 2004, [^{18}F]Galacto-RGD[113] was the first RGD conjugated with FDG to achieve heterologous dual-targeting, after which it was further rationally modified to obtain [^{18}F]F-RGD-K5 (**63**) (Figure 10).[114] [^{18}F]F-RGD-K5 has a similar biodistribution in monkeys and humans; increased uptake in the bladder, liver and kidneys; and rapid clearance through the renal system. Studies have shown that [^{18}F]F-RGD-K5 can be safely used to image $\alpha_v\beta_3$ integrin expression in humans.

3.2.7. $\alpha_v\beta_3$-CD13 Dual-targeted Radiopharmaceuticals. The expression levels of $\alpha_v\beta_3$ and CD13 in serum and tumor tissues are associated with tumor type, angiogenesis, invasiveness, metastasis, and overall survival, thus serving as indicators of a poor prognosis in cancer.[115] Effective assessment of their expression levels can facilitate the monitoring of cancer progression and aid in the development of treatment strategies. The $\alpha_v\beta_3$ and CD13 dual-targeted tracer [^{68}Ga]Ga-NGR-RGD (**64**)[116] was prepared by conjugating RGD and Asp-Gly-Arg (NGR). PET/CT images revealed that [^{68}Ga]Ga-NGR-RGD

https://doi.org/10.1021/acs.jmedchem.4c01608
J. Med. Chem. 2024, 67, 21644−21670

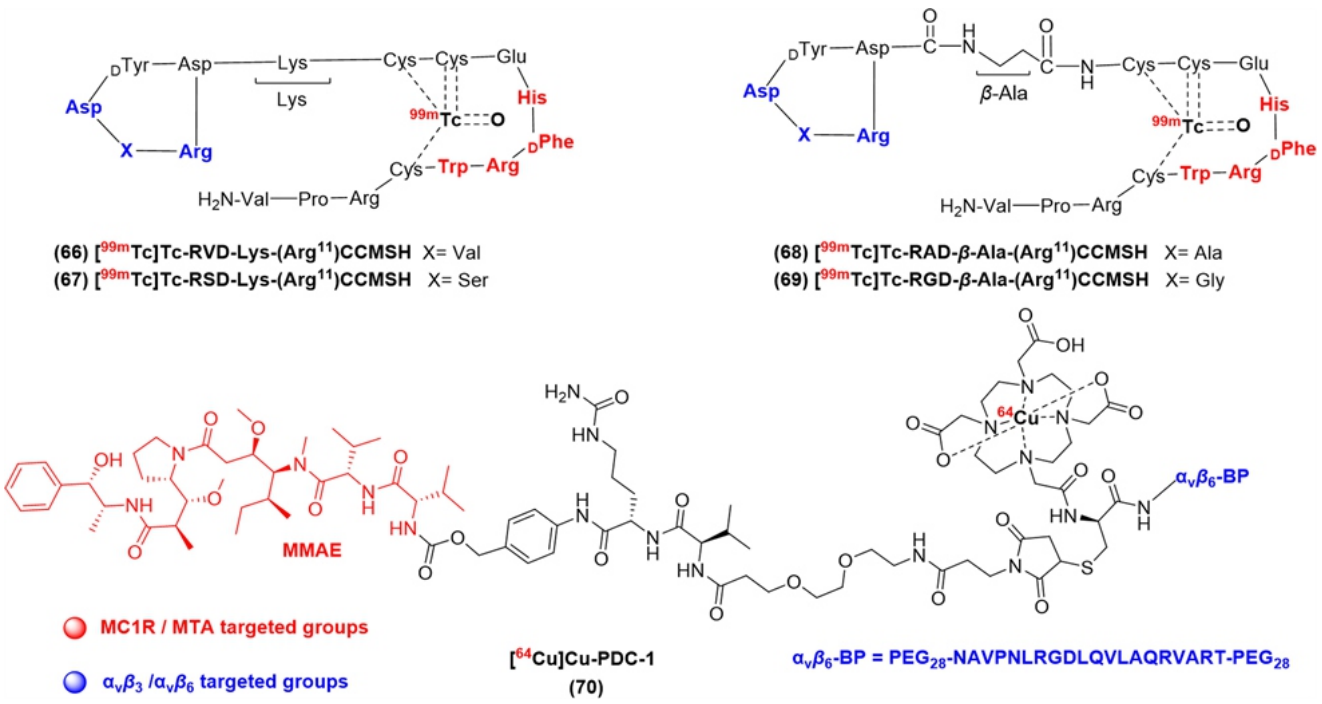

Figure 11. $\alpha_v\beta_3$-MC1R and $\alpha_v\beta_6$-MTA dual-targeted radiopharmaceuticals.

was clearly visible in the MCF-7 mouse model and showed greater uptake than did [^{68}Ga]Ga-RGD or [^{68}Ga]Ga-NGR alone at 0.5 h after injection. At the same time, lung metastatic lesions were clearly detected in a mouse model of lung metastasis. Compared with [^{68}Ga]Ga-RGD or [^{68}Ga]Ga-NGR, [^{68}Ga]Ga-NGR-RGD showed greater binding affinity, targeted efficiency, and longer tumor retention times. Its better pharmacokinetic properties make it an ideal candidate for future clinical evaluation of $\alpha_v\beta_3$- and CD13-positive patients.

3.2.8. $\alpha_v\beta_3$-CXCR4 Dual-targeted Radiopharmaceuticals. Chemokine (C-X-C motif) receptor 4 (CXCR4) and integrin $\alpha_v\beta_3$ are involved in several key biological processes in cancer and have been extensively studied as molecular imaging targets.[117] The overexpression of CXCR4 leads to tumor growth, invasion, angiogenesis, metastasis, recurrence, and drug resistance and is associated with an overall poor prognosis.[118] Compared with the MX-1 (CXCR4-, $\alpha_v\beta_3$-) mice model, heterodimer tracer [^{68}Ga]Ga-yG5-RGD (**65**),[119] which is a dual-targeted CXCR4 and $\alpha_v\beta_3$ tracer, accumulated at high concentrations in BxPC3 (CXCR4+, $\alpha_v\beta_3$+) tumors and was effectively blocked, confirming its dual receptor-targeted properties. These findings indicate that [^{68}Ga]Ga-yG5-RGD can be used for noninvasive detection of tumors expressing CXCR4, integrin $\alpha_v\beta_3$ or both and is a promising tracer. Therefore, potentially good prospects for clinical application.

3.2.9. $\alpha_v\beta_3$-MC1R Dual-targeted Radiopharmaceutical. Malignant melanoma is the deadliest form of cancer, and overexpression of the melanocortin-1 receptor (MC1R) and the $\alpha_v\beta_3$ integrin receptor on melanoma cells is an attractive molecular target for drug development.[120] α-Melanocyte-stimulating hormone (α-MSH) peptides are widely used to target MC1R for melanoma imaging, and a dual receptor-targeting imaging tracer that combines $\alpha_v\beta_3$ with MC1R for melanoma imaging represents a potential strategy represents.[121,122] Both [^{99m}Tc]Tc-RVD-Lys-(Arg^{11})CCMSH (**66**)[123] and [^{99m}Tc]Tc-RSD-Lys-(Arg^{11})CCMSH (**67**)[124] showed good affinity properties in B16/F1 melanoma cells, with the maximum tumor uptake (19.63 ± 4.68% ID/g, 4 h; 18.01 ± 4.22% ID/g, 0.5 h, respectively) and the kidney is the highest uptake organ (94.01 ± 18.31 and 80.01 ± 15.67% ID/g, 2 h). Compared to [^{99m}Tc]Tc-RVD-Lys-(Arg^{11})CCMSH, [^{99m}Tc]Tc-RSD-Lys-(Arg^{11})CCMSH has faster clearance in the kidney, and Ser modification appears to be more beneficial in nontarget organ clearance as Val. The high uptake in the kidneys limits the contrast of SPECT/CT images, and reducing tracer accumulation in the kidneys is a research focus for the heterologous dual-targeted $\alpha_v\beta_3$-MC1R. [^{99m}Tc]Tc-RAD-β-Ala-(Arg^{11})CCMSH (**68**)[125] and [^{99m}Tc]Tc-RGD-β-Ala-(Arg^{11})CCMSH (**69**)[126] adjusted the linker in the targeting group (β-Ala replaced Lys), resulting in a significant reduction in the kidney retention (20.18 ± 3.86% ID/g and 16.31 ± 4.60% ID/g, 2 h) and yet high uptake within the tumor (15.66 ± 6.19% ID/g, 2 h; 17.98 ± 2.49% ID/g, 4 h, respectively). B16/F1 melanoma lesions can be clearly visualized on SPECT/CT images. In the development of the $\alpha_v\beta_3$-MC1R heterodimer tracers, it can be seen that the linker-based modification strategy appears to be more effective than cyclic RGD peptide modification in eliminating nontarget organs. Compared to Lys, β-Ala has a significant advantage in reducing renal uptake. [^{99m}Tc]Tc-RGD-β-Ala-(Arg^{11})CCMSH needs to be compared head to head with the corresponding monomer to further validate the advantages of heterodimer over monomer.

3.2.10. $\alpha_v\beta_6$-MTA Dual-targeted Radiopharmaceutical. Integrin $\alpha_v\beta_6$ is an epithelial-specific cell surface receptor that is expressed at low levels in healthy adult epithelia but is highly expressed in many cancers and is involved in cell invasion, migration, angiogenesis, and extracellular matrix adhesion.[127] Importantly, it has been identified as a prognostic marker, with high expression levels correlating with a poor patient prognosis and short overall survival. $\alpha_v\beta_6$-binding peptide ($\alpha_v\beta_6$-BP) is a peptide that binds to integrin $\alpha_v\beta_6$ with nanomolar affinity and high selectivity. [^{18}F]F-$\alpha_v\beta_6$-BP has been translated into the

https://doi.org/10.1021/acs.jmedchem.4c01608
J. Med. Chem. 2024, 67, 21644−21670

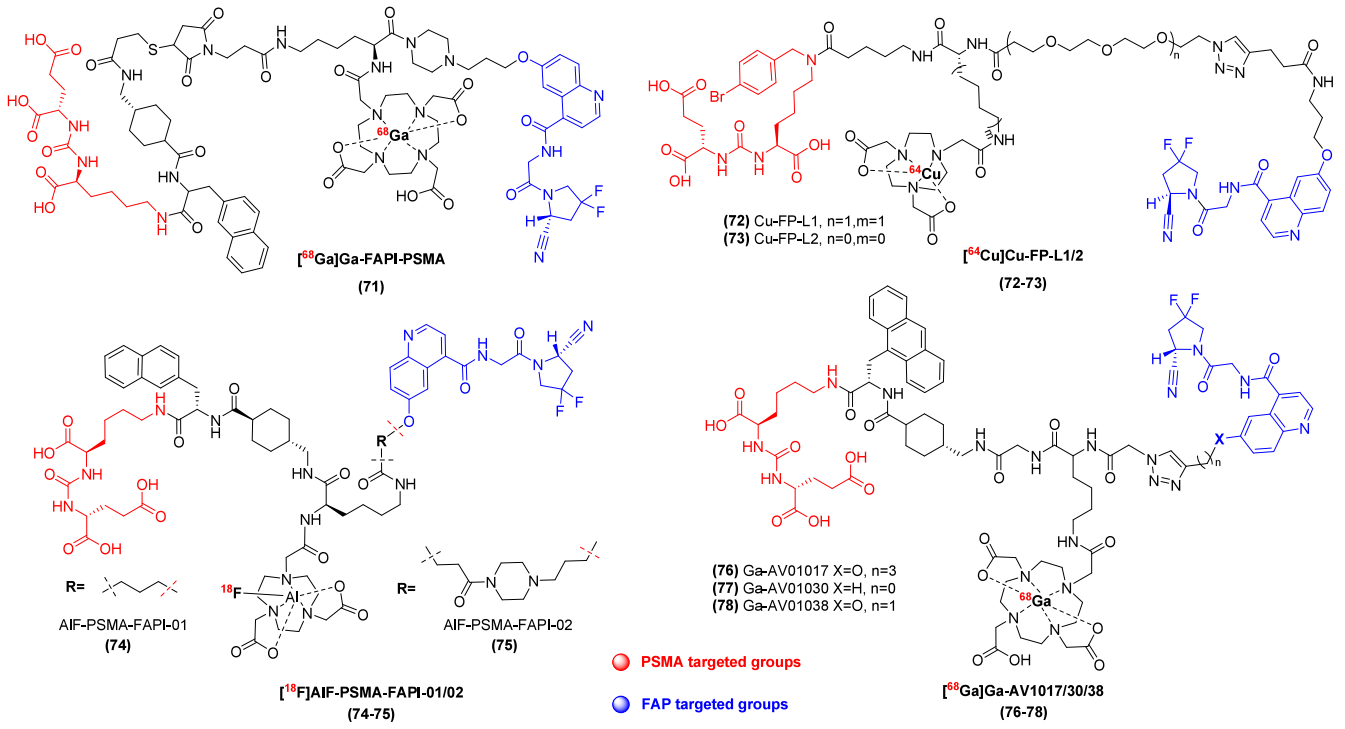

Figure 12. FAP-PSMA dual-targeted radiopharmaceuticals.

clinic for the detection of tumors in patients with breast, colon, lung, and pancreatic cancer.[128] Peptide−drug conjugates (PDCs) constitute an important type of drug research that usually consists of three parts: targeted groups, cytotoxic groups, and linkers.[129] The development of radiolabeled PDC-integrated diagnostic and treatment drugs has important clinical application value. The $\alpha_v\beta_6$-microtubule targeting agent (MTA) heterologous dual-targeted tracer [^{64}Cu]Cu-PDC-1 (**70**)[130] was prepared by conjugating $\alpha_v\beta_6$-BP and monomethyl auristatin E (MMAE). MMAE is a potent MTA, several MMAE-based targeted tumor drugs have been successfully used in clinical practice (Figure 11).[129] It was clearly visible in the tumors of $\alpha_v\beta_6$ positive DX3puroβ_6 and BxPC3 mouse models, but no significant uptake was observed in the DX3pro ($\alpha_v\beta_6$-) tumors. The biodistribution results revealed that the tumor uptake of X3puroβ_6 was 8 times greater (4.46 vs 0.56% ID/g) than that of DX3puro at 4 h after injection. In vivo therapeutic efficacy studies revealed that the cytotoxic MMAE group exhibited good antitumor effects. Compared with that of the control group, the overall survival rate of the DX3puroβ_6 mouse model increased by more than 2-fold. [^{64}Cu]Cu-PDC-1 successfully achieved selective accumulation and visualization of integrin $\alpha_v\beta_6$ in tumors and had good pharmacokinetic characteristics. This was a successful exploration of integrated radiopharmaceuticals for the diagnosis and treatment of PDC types, expanding the design strategies and providing important guidance for the development of subsequent PDC radiopharmaceuticals.

Overall, the design of integrin heterologous dual-targeted radiopharmaceuticals, such as [^{68}Ga]Ga-FAPI-RGD, [^{68}Ga]Ga-NOTA-RGD-BBN, and [^{68}Ga]Ga-LNC1015, is a reasonable and effective strategy and these molecules have shown good clinical application prospects. Therefore, the use of integrin as a secondary target is an important direction for the development of heterologous dual-targeted radiopharmaceuticals.

3.3. Other Dual-targeted Radiopharmaceuticals.

3.3.1. FAP-PSMA Dual-targeted Radiopharmaceuticals. With the widespread clinical application of radiotracers for PSMA and FAP, heterodimeric tracers that target two targets simultaneously have also been widely studied in recent years. [^{68}Ga]Ga-FAPI-PSMA (**71**)[131] has a relatively high affinity for PSMA and FAP, with IC_{50} values of 4.73 and 2.10 nM, respectively. It rapidly accumulated in the tumors of 22Rv1 and U87MG model mice, and high-contrast PET images were obtained within 1 h of injection. By adjusting the length of the linker, [^{64}Cu]Cu-FP-L1 (**72**) and [^{64}Cu]Cu-FP-L2 (**73**)[132] were obtained, both of which have affinities for FAP and PSMA proteins in the nanomolar range (Figure 12). Notably, the targeted groups of PSMA and FAP are both nonclassical. PET imaging and biodistribution studies revealed that [^{64}Cu]Cu-FP-L1 exhibited more favorable pharmacokinetic properties than did [^{64}Cu]Cu-FP-L2. In the U87MG mouse model, [^{64}Cu]Cu-FP-L1 showed comparable tumor uptake to [^{64}Cu]Cu-FAPI-04 and showed a clear advantage in retention within the tumor, and the same trend was observed in PC3 PIP tumors. [^{68}Ga]Ga-FAPI-PSMA and [^{64}Cu]Cu-FP-L1 showed highly specific tumor-targeting to FAP and PSMA and were able to be used to image lesions expressing FAP, PSMA, or both on the surface of tumor cells or in the tumor microenvironment, which has important clinical application prospects.

[^{18}F]AlF-PSMA-FAPI-01 (**74**) and [^{18}F]AlF-PSMA-FAPI-02 (**75**)[133] showed nanomolar affinities for both the PSMA and FAP proteins. Compared with monospecific tracers, these two ^{18}F-labeled heterodimers showed better tumor uptake in A549-FAP (FAP+) and 22Rv1 mouse models. However, their high uptake in nontarget organs remains a concern, especially in the kidneys and bones. Notably, the high uptake in the bones can be blocked by the competitive inhibitor DOTA-FAPI-04 and is not due to the pharmacokinetic properties of fluorine atom detachment. The broad spectrum and mature clinical

https://doi.org/10.1021/acs.jmedchem.4c01608
J. Med. Chem. 2024, 67, 21644−21670

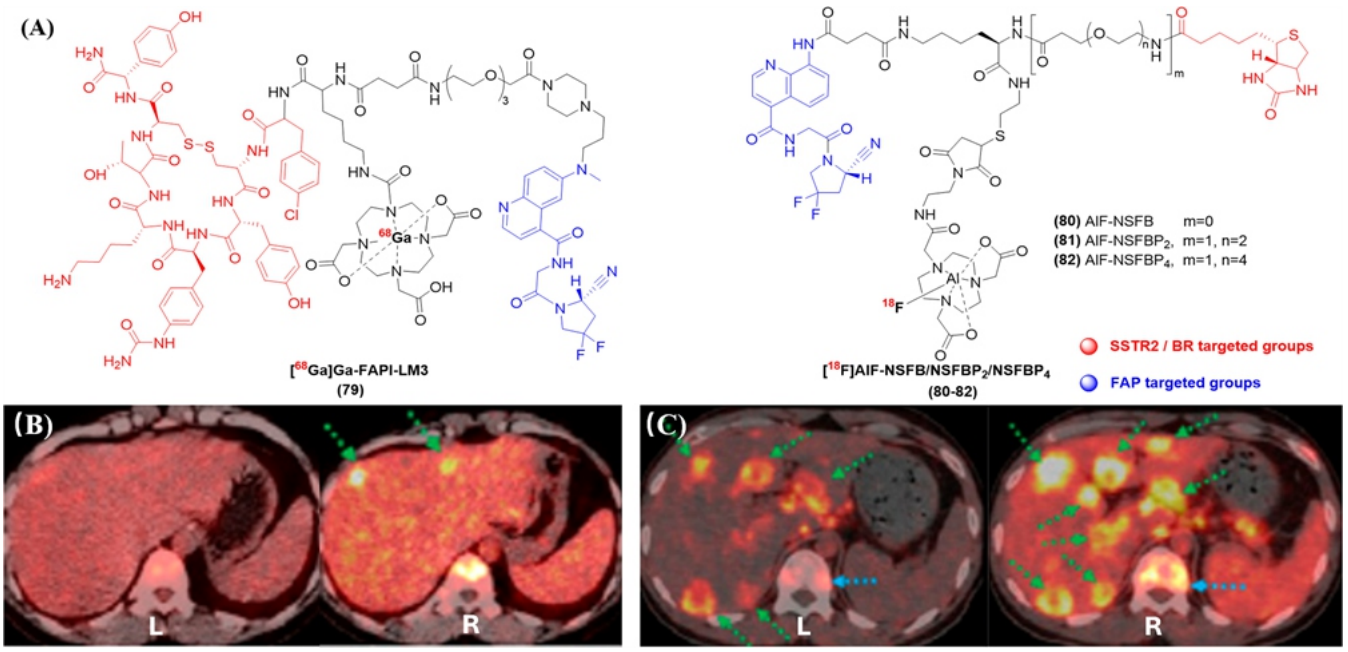

Figure 13. FAP-SSTR2 and FAP-BR dual-targeted radiopharmaceuticals. (A) Structure of FAP-SSTR2 and FAP-BR dual-targeted radiopharmaceuticals; (B) [^{18}F]FDG (L) and [^{68}Ga]Ga-FAPI-LM3 (R) PET/CT images of a patient with nasopharyngeal carcinoma and (C) is [^{68}Ga]Ga-FAPI-46 (L) and [^{68}Ga]Ga-FAPI-LM3 (R). Figures B and C were reprinted with permission from ref 138. Copyright SNMMI.

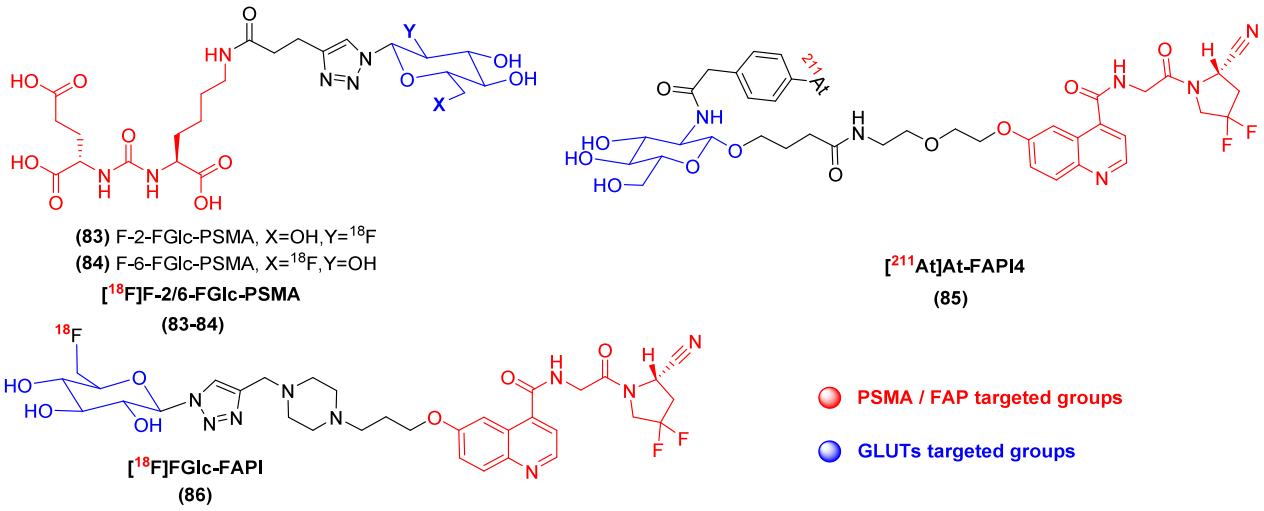

Figure 14. GLUTs-PSMA and GLUTs-FAP dual-targeted radiopharmaceuticals.

applications of ^{18}F make it easier to promote, and it is a potential FAP-PSMA dual-targeted radiotracer.

However, not all integration strategies are effective. The three FAP-PSMA heterologous dual-targeted tracers [^{68}Ga]Ga-AV01017 (**76**), [^{68}Ga]-Ga-AV01030 (**77**) and [^{68}Ga]Ga-AV01038 (**78**)[134] showed uniform tumor uptake in both the LNCaP and HEK293T (FAP+) mouse models that was significantly lower than of the corresponding monospecific tracers. Although the three heterodimers labeled with ^{68}Ga show good affinity for FAP (IC_{50} = 1.25−2.74 nM) and PSMA (IC_{50} = 25.2−71.6 nM) in vitro, their pharmacokinetic properties are unsatisfactory. Once again, it is shown that the affinity and pharmacokinetic properties are not completely consistent, which also means that the method of screening lead radiotracers by affinity is not completely effective.

3.3.2. FAP-SSTR2 Dual-targeted Radiopharmaceuticals. In recent years, the SSTR2-targeted properties of LM3 and JR11 have been extensively studied.[135,136] Unlike SSTR2 agonists, which exhibit high internalization rates, the antagonist LM3 has high binding affinity for SSTR2. LM3 is characterized by low hepatic uptake and lesions with better background contrast, showing good potential for peptide receptor radionuclide therapy.[137] Heterodimer tracer [^{68}Ga]Ga-FAPI-LM3 (**79**)[138] showed high affinity for both FAP and SSTR2. In the HT-1080-FAP and HT-1080-SSTR2 mouse models, the tumor uptake of [^{68}Ga]Ga-FAPI-LM3 was significantly greater than that of monomeric [^{68}Ga]Ga-FAPI-46 and [^{68}Ga]Ga-DOTA-LM3. In a study of 6 clinical nasopharyngeal carcinoma patients, as shown in Figure 13 B and 13 C, [^{68}Ga]Ga-FAPI-LM3 PET/CT showed significant advantages over [^{18}F]FDG and [^{68}Ga]Ga-FAPI-46 in primary and metastatic lesions, enhancing lesion detectability

https://doi.org/10.1021/acs.jmedchem.4c01608
J. Med. Chem. 2024, 67, 21644−21670

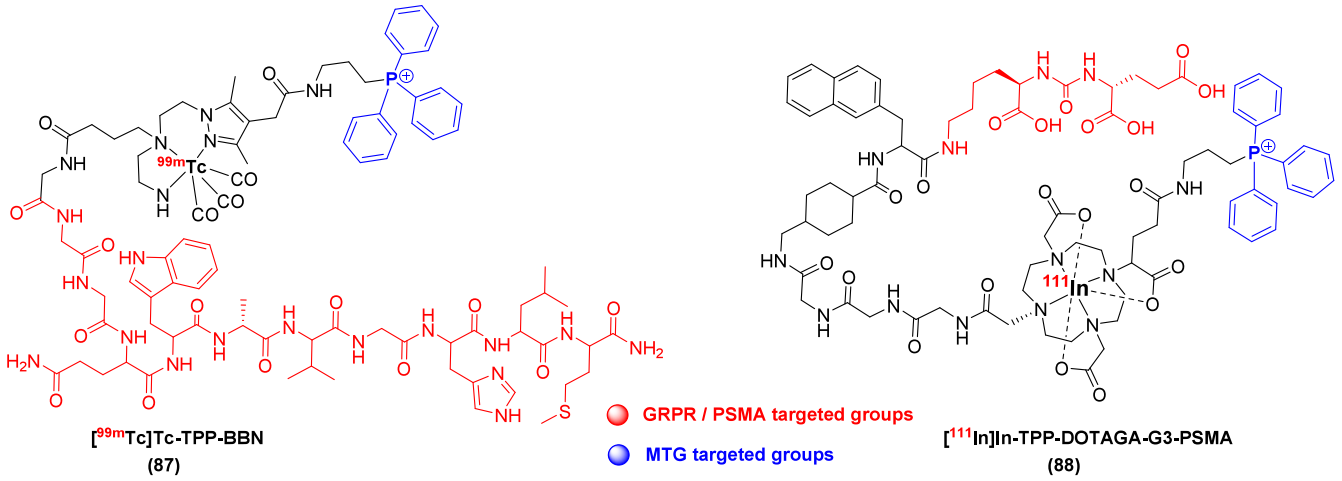

Figure 15. MTG- GRPR and MTG-PSMA dual-targeted radiopharmaceuticals.

and tumor identification. Overall, the results of [^{68}Ga]Ga-FAPI-LM3 demonstrate its clinical feasibility for PET/CT imaging in patients with nasopharyngeal carcinoma.

3.3.3. FAP-BR Dual-targeted Radiopharmaceuticals. Biotin receptors (BR) are overexpressed in many tumors and are important targets for the development of broad-spectrum antitumor drugs.[139] Although the radiopharmaceuticals developed on the basis of BR have limited effects, recent studies have shown that their combination with antibiotin can enhance their imaging effect.[140] Therefore, the development of biotin heterodimer radiotracers is an effective strategy to address the shortcomings of monomers. Among the three FAP-BR dual-targeted radiotracers (**80**−**82**),[141] [^{18}F]AlF-NSFBP$_4$ (**82**) showed the most powerful pharmacokinetic characteristics. In terms of the relationship between the structure and pharmacokinetic properties of the three drugs, the introduction of PEG chains is necessary, and the presence and length of PEG chains are positively correlated with the clearance of the tracers from nontarget organs and the absolute uptake of tumors. Compared with the FAP-targeted monomer [^{18}F]AlF-NSF (without biotin), [^{18}F]AlF-NSFBP$_4$ showed high uptake and TBRs in tumors. More importantly, it still had good diagnostic performance in mouse models with low FAP expression, which has positive significance for the diagnosis of early tumors (especially when FAP has not yet formed in the tumor microenvironment or when its expression on CAFs has not increased). Therefore, [^{18}F]AlF-NSFBP$_4$ is expected to become a candidate for further clinical translational research.

3.3.4. GLUTs-PSMA Dual-targeted Radiopharmaceuticals. The [^{18}F]2-FGlc-PSMA (**83**) and [^{18}F]6-FGlc-PSMA (**84**)[142] were prepared to investigate the effect of heterodimer formation between GLUTs and PSMA on the tumor binding ability and in vivo clearance behavior of the radiotracer (Figure 14). Both showed moderate affinities for PSMA, [^{18}F]2-FGlc-PSMA and [^{18}F]6-FGlc-PSMA, with 2- to 3-fold greater uptake in the PC3-PIP mouse model than in the [^{68}Ga]Ga-PSMA-11 PET scans. Both radiotracers are cleared only through the kidneys rather than through the hepatobiliary pathway, and [^{18}F]6-FGlc-PSMA has a 10-fold faster renal clearance rate than [^{18}F]2-FGlc-PSMA does. Therefore, [^{18}F]6-FGlc-PSMA has fairly low renal uptake and rapid clearance, exhibits high uptake in PSMA-positive tumors in vivo, and deserves further clinical study.

3.3.5. GLUTs-FAP Dual-targeted Radiopharmaceuticals. ^{211}At radionuclide to label GLUTs and FAP to form heterodimers [^{211}At]At-FAPI4 (**85**)[143] to explore the effect on the performance of the FAP tracer. There were significant differences in the uptake of [^{211}At]At-FAPI4 between parental and FAP-overexpressing tumor cells (A549/HEK293), proving that it is specific for FAP, and its pharmacokinetics and imaging properties have not been studied. The GLUTs-FAP dual-targeted radiotracer [^{18}F]FGlc-FAPI (**86**)[144] has good application prospects. Compared with FAPI-04, FGlc-FAPI has a slightly lower affinity (IC_{50} = 32 nM vs 167 nM) for FAP in vitro, but its tumor uptake in the HT1080-FAP and U87MG mouse models is greater than that of [^{68}Ga]Ga-FAPI-04, and it has a higher tumor retention rate. The incomplete unification of affinity and pharmacokinetics was once again demonstrated. Interestingly, PET images revealed that [^{18}F]FGlc-FAPI has high specific uptake in bone structures and joints, indicating that it may be used for the diagnosis of FAP-related diseases other than tumors, such as arthritis, heart disease or pulmonary fibrosis. The heterologous dual-targeted radioactive tracer [^{18}F]FGlc-FAPI shows promising advantages in the diagnosis of FAP-related diseases and deserves further study, but its complex and cumbersome labeling method still needs to be further optimized to facilitate clinical promotion.

3.3.6. MTG-GRPR Dual-targeted Radiopharmaceuticals. Targeting mitochondrial Auger electron-emitting radioconjugates is an attractive strategy in tumor radiotherapy because mitochondrial DNA is damaged by exposure to ionizing radiation and cannot be repaired efficiently compared with nuclear DNA, and the irradiation of mitochondria can also induce other harmful effects, such as reactive oxygen species production or apoptosis.[145−147] Triphenylphosphonium (TPP) derivatives are potent mitochondrial targeting groups (MTG).[148] MTG-GRPR dual-targeted radiotracer [^{99m}Tc]Tc-TPP-BBN (**87**)[149] enhanced the aggregation of ^{99m}Tc in the mitochondria of target tumor cells in a dose-dependent manner (Figure 15). This method significantly reduced the survival and proliferation ability of PC-3 cells.

3.3.7. MTG-PSMA Dual-targeted Radiopharmaceuticals. ^{99m}Tc has a relatively low Auger electron yield and is not an ideal Auger electron emitter,[145] ^{111}In-labeled MTG-PSMA heterologous dual-targeted radiotracer [^{111}In]In-TPP-DOTA-G3-PSMA (**88**)[150] showed similar binding affinity to PSMA as [^{111}In]In-PSMA-617 and impaired cell survival in a dose-dependent manner, with higher cytotoxicity than the single targeted homologue [^{111}In]In-PSMA-617. The TPP pharmaco-

https://doi.org/10.1021/acs.jmedchem.4c01608
J. Med. Chem. 2024, 67, 21644−21670

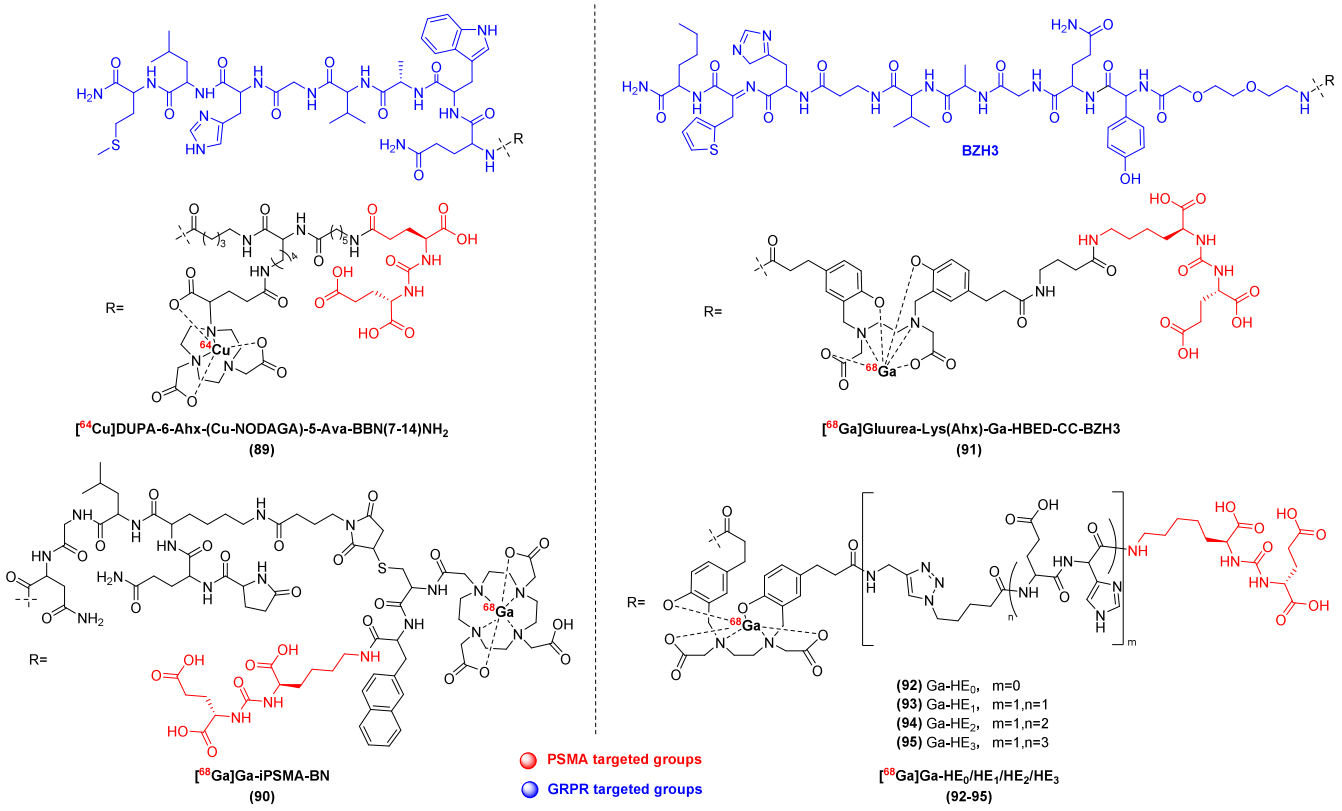

Figure 16. GRPR-PSMA dual-targeted radiopharmaceuticals.

phore does not interfere with the SPECT imaging quality of [^{111}In]In-TPP-DOTAGA-G3-PSMA in a PCa mouse model. Research on [^{111}In]In-TPP-DOTAGA-G3-PSMA provides valuable insights into the potential use of Auger electron-emitting radionuclides in radiotherapy and may extend research to other trivalent Auger electron-emitting radionuclide metals (such as ^{161}Tb or ^{165}Er), thus opening new paths for the application of radionuclides in the field of tumor treatment.

3.3.8. GRPR-PSMA Dual-targeted Radiopharmaceuticals. The radiotracer [^{64}Cu]DUPA-6-Ahx-(Cu-NODAGA)-5-Ava-BBN (7−14) NH_2 (**89**)[151] represents the first attempt at dual-targeted of GRPR-PSMA and shows good receptor binding ability in PC-3 (GRPR+) and LNCaP cells with IC_{50} values of 11.1 ± 0.46 nM and 1.16 ± 1.35 nM, respectively. The biodistribution study in the PC-3 model showed that the tracer was mainly excreted via the kidneys and had high accumulation in the small intestine. Although tumor uptake was observed, PET images in both PC-3 and LNCaP models did not show superior performance compared to the corresponding monomers. [^{68}Ga]Ga-iPSMA-BN (**90**)[152] was adjusted the linker and used DOTA as the metal chelator. The uptake in PC-3 and LNCaP cells is significantly higher than that of the corresponding monomer and is excreted via the renal metabolic system, effectively reducing intestinal uptake. PET imaging indicates good accumulation at PCa lesion sites. Pharmacokinetic and dosimetric measurements were performed in four volunteers with an average effective dose of 2.70 ± 0.05 mSv and a rapid blood clearance rate ($t_{1/2}$ = 2.64 min).[153] It is worth further clinical investigation to determine that [^{68}Ga]Ga-iPSMA-BN is more likely to detect lesions that are difficult to detect with [^{68}Ga]Ga-iPSMA.

[^{68}Ga]Gluurea-Lys(Ahx)-Ga-HBED-CC-BZH3 (**91**)[154] was a GRPR-PSMA heterodimeric tracer prepared by using BZH3 as a GRPR targeting agent and HBED-CC (*N*,*N*′-Bis-[2-hydroxy-5-(carboxyethyl)benzyl]ethylenediamine-*N*,*N*′-diacetic acid) as a metal chelator, with affinity for PSMA and GRPR proteins similar to that of the corresponding monomer. Biodistribution studies have shown that [^{68}Ga]Gluurea-Lys(Ahx)-Ga-HBED-CC-BZH3 exhibits dual targeting for PSMA (5.4% ID/g, PSMA +) and GRPR receptors (3.3% ID/g, GRPR+), with high uptake in the kidneys and spleen. The introduction of amino acid linker (-His-Glu-)$_{0-3}$ between metal chelator and PSMA targeting group of [^{68}Ga]Ga-HE_0/HE_1/HE_2/HE_3 (**92**−**95**)[155] effectively reduces uptake in nontarget organs, particularly the kidneys (Figure 16). All four tracers effectively target PSMA and GRPR on LNCaP and PC-3 cells and tumor xenografts. [^{68}Ga]Ga-HE_2 (**94**) has the maximum tumor uptake (3.68 ± 0.43% ID/g in PC3 model, 10.66 ± 4.19% ID/g in LNCaP model) and TBRs. Although the use of the (-His-Glu-)$_2$ amino acid linker effectively improves the pharmacokinetic properties of the tracer, it is worth noting that the presence or absence of the linker and its length do not have a clear linear relationship with the pharmacokinetic improvement. And each of these should be considered a unique situation, as even minor changes in the linker region can have significant effects on pharmacokinetics.

3.3.9. PD-L1-CTLA-4 Dual-targeted Radiopharmaceuticals. Immunotherapy involving immune checkpoint blockade, especially combination therapy targeting programmed cell death inhibitor 1 (PD-1) or its ligands (programmed apoptosis ligand 1, PD-L1) and cytotoxic T lymphocyte-associated protein 4 (CTLA-4), has a significant effect on the prognosis of patients with malignant melanoma.[156] To address the limitations of immunotherapy, bispecific fusion antibodies have been developed for the treatment of malignant melanoma.[157] KN046 can show good therapeutic effects by binding to PD-L1 and CTLA-4 while reducing side effects and treatment costs

https://doi.org/10.1021/acs.jmedchem.4c01608
J. Med. Chem. 2024, 67, 21644−21670

due to its simplified structure.[158] Despite the important advantages of bispecific fusion antibodies, there is still an urgent need to effectively identify patients who benefit from PD-L1/CTLA-4 immunotherapy.[159] Radionuclide therapy is a promising platform for nuclear medicine imaging and cancer treatment. The ^{131}I-labeled heterologous dual-targeted fusion antibody [^{131}I]I-KN046 (**96**)[159] can simultaneously target PD-L1-CTLA-4. The tracer has high affinity and specificity for PD-L1/CTLA-4 immune targets and has good in vivo tumor retention, thereby achieving good antitumor effects. More importantly, the combination of low-dose ^{131}I and KN046 enhances immune sensitivity and significantly improves the response rate to immunotherapy. The design strategy of [^{131}I]I-KN046 will expand the application of nuclear oncology in immunotherapy and create more opportunities for cancer therapy. In the future, the use of radioactive metal nuclide-conjugated fusion antibodies will become an important component of the field of radiopharmaceutical research (Figure 17).

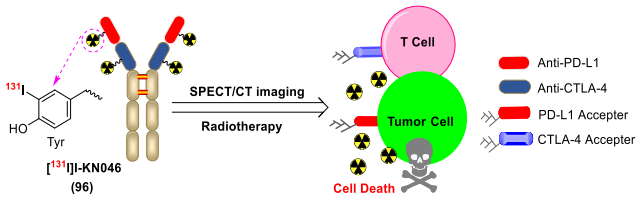

Figure 17. PD-L1-CTLA-4 dual-targeted radiopharmaceuticals.

In general, compared with studies on heterologous dual-targeted radiopharmaceuticals targeting ALB and integrin, there are fewer studies on dual-targeted radiopharmaceuticals with other heterologous target combinations. But they still show great application potential in clinical applications (such as [^{68}Ga]Ga-DOTA-LM3), which greatly broadens the research direction (such as radioimmunotherapy) of radiopharmaceuticals. With the increasing maturity of bispecific fusion antibodies, more target combinations will enter the development and application of heterologous dual-targeted radiopharmaceuticals, it will be a hot topic in the future research of radiopharmaceuticals.

4. APPLICATION OF CADD IN THE DESIGN OF HETEROLOGOUS DUAL-TARGETED RADIOPHARMACEUTICALS

In recent years, attribute-based drug design has attracted considerable attention and is considered a potential candidate for the Nobel Prize.[160−162] Computer-aided drug design (CADD) technology plays an important role here. Compared with traditional experimental methods, it can simulate the interaction between molecules and targets, reduce the blindness of experiments, and significantly shorten the time and cost of drug development. Molecular docking (MD) and molecular dynamics simulation (MDS) have become common tools in modern drug discovery.[163−167] Through the above-mentioned analysis of the structural design of heterologous dual-targeted radiopharmaceuticals, it is not difficult to find that small changes between structures have a huge impact on the performance of tracers, and general universal rules are difficult to summarize. The structural design of each tracer may need to be considered independently. Using MD and MDS tools to validate the rationality of heterologous dual-targeted tracer design could be a promising approach. When designing [^{68}Ga/^{177}Lu]Ga/Lu-FSDD$_0$/$_1$/$_3$I (**37**−**39**), the rationality of the tracer design was theoretically verified by MD. For FAP protein, the docking scores of the three tracers were comparable to FAPI-04 (−12.93, −14.36, −13.70 vs −12.56 kcal/mol), indicating that the introduction of IPBA has no influence on the binding to the FAP protein. Compared to FAPI-04, the three tracers also have significant advantages in binding to ALB (−4.07 vs −12.25, −11.68, −10.57 kcal/mol).[81] Compared to experimental results (FSDD$_0$ has the best performance), improving binding to ALB appears to be more beneficial for tracer performance. [^{18}F]AlF-NSFB/NSFBP2/NSFBP4 (**80**−**82**) also theoretically confirmed the binding of four tracers to FAP protein in MD and MDS (−10.02, −11.20, −13.27 vs −13.74 kcal/mol).[141] The performance of [^{18}F]AlF-NSFBP4 in the experiment was consistent with the trend of theoretical screening. EB-FAPI-B1(**40**) and FAPI-02 have the same affinity potential for FAP protein (−12.56 vs −12.26 kcal/mol), and the binding affinity between EB-FAPI-B1 and ALB is significantly better than that of FAPI-02 (−14.11 vs −5.65 kcal/mol),[83] it has entered phase I clinical trials. It can be seen that MD and MDS are helpful to verify the rationality of molecular structure design. As shown in Figure 18, binding heterodimeric tracers to two corresponding targets can verify the rationality of the molecular structure. At the same time, the synergy between targets and key features in the drug structure can also be verified, providing a direction for future improvement of tracer performance. At the same time, the stable protein−ligand complex conformation calculated by MDS and energy calculation provide valuable insights into the binding mechanisms between proteins and ligands It is envisaged that theoretical research on proteins and ligands will effectively reduce blindness in structure design, especially by achieving high-throughput combination and screening of

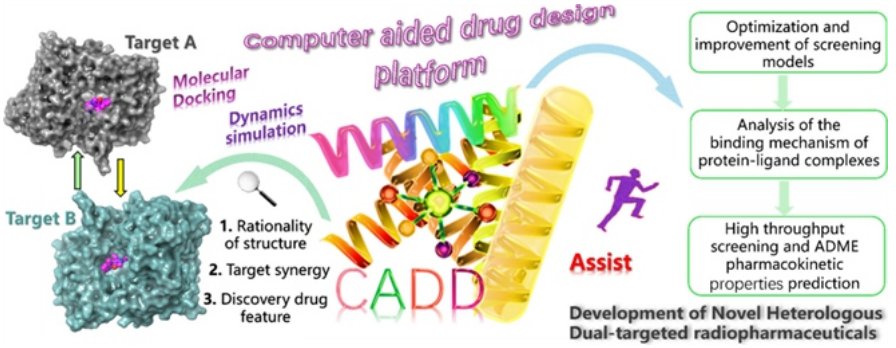

Figure 18. Application of CADD in the design of heterogeneous dual-targeted radiopharmaceuticals.

https://doi.org/10.1021/acs.jmedchem.4c01608
J. Med. Chem. 2024, 67, 21644−21670

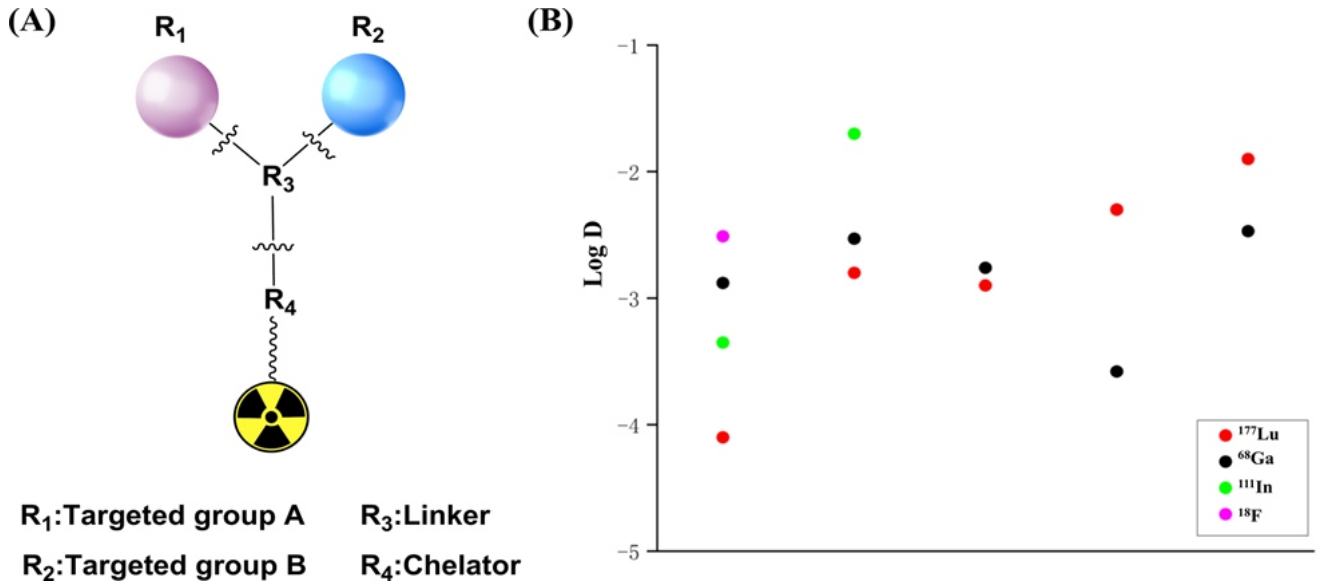

Figure 19. SAR of heterologous dual-targeted radiopharmaceuticals. (A) General formula for SAR; (B) Log *D* of potential heterologous dual-targeted radiopharmaceuticals.

structures under various constraints (e.g., control of bond length, bond angle, specific amino acid, different interaction forces, etc.) and improves the efficiency of the development of dual-targeted radiopharmaceuticals. In addition, prediction of absorption, distribution, metabolism and excretion (ADME) properties based on structure will also open a new perspective for tracer screening. Multidimensional comprehensive evaluation of tracer performance at the theoretical level is an effective strategy to improve the development of heterologous dual-targeted radiopharmaceuticals. However, the rationality of the verification method and the reliability of the model are the guarantees for obtaining valuable screening results, which need to be optimized and confirmed through repeated verification of the theory combined with experiments.

5. SAR OF HETEROLOGOUS DUAL-TARGETED RADIOPHARMACEUTICALS

The structure−activity relationships (SAR) of all of the above heterologous dual-targeted radiopharmaceuticals are summarized in Figure 19A. Owing to the diversity of the four group structures, each group structure cannot be accurately divided, but the relationships among the four groups are still clear. First, the targeted group (R1, R2) is usually classical, and its change is not necessary. Undoubtedly, the modification of the R1 and R2 groups increases the diversity of the molecule, but it also increases the affinity of the corresponding target. The second is the linker (R3) between the targeted groups. Through the discussion of the SAR of the R3 group of heterologous dual-targeted radiopharmaceuticals in this paper, its effect on pharmacokinetics is not linear, which means that the rational selection and optimization of R3 is the key to the development of heterologous dual-targeted radiopharmaceuticals. Moreover, the linker is crucial for regulating the lipid−water partition coefficient of the entire molecular system. Appropriate lipid−water partitioning guarantees pharmacokinetic performance,[168] similar to the drug−like principle of general drugs. At present, the field of radiopharmaceuticals has not summarized a regular drug-making principle. We attempted to summarize the regularity of the lipid−water distribution of the above-mentioned potential heterologous dual-targeted radiopharmaceuticals (Figure 19B) and found that a Log *D* between −2 and −4 may be beneficial to pharmacokinetics and that there may be differences in the lipid−water distributions of radioactive therapeutic drugs and diagnostic drugs. Unfortunately, owing to the small sample size, a clearer correlation may not be obtained, which is also worthy of attention in subsequent studies of dual-targeted radiopharmaceuticals. Metal chelators (R4) are also usually classic, such as DOTA, NOTA and their corresponding derivatives. Notably, although R4 has rich coordination functions (a chelator can coordinate multiple radionuclides), this does not mean that radiometal nuclides can be equivalently replaced. The difference after coordination of different nuclides is obvious. Therefore, although the relationships among the four groups are clear, the new molecules formed by their combination are full of uncertainty. Studying heterologous dual-targeted radiopharmaceuticals from a comprehensive perspective of the overall molecular structure is crucial.

6. PERSPECTIVES AND CONCLUSIONS

The advancement of heterologous dual-targeted radiopharmaceuticals represents a vibrant and rapidly progressing field of research, offering substantial promise for the diagnosis and therapeutic management of associated receptors and diseases, thereby catalyzing the swift growth of nuclear medicine. It is exciting that some heterologous dual-targeted radiopharmaceuticals have yielded satisfactory results, confirming the theoretical rationality and clinical feasibility of the combination of targets. These successes have established a robust theoretical framework and provided practical insights for the continued development of additional heterologous dual-targeted radiopharmaceuticals. There is no doubt that the development of heterologous dual-targeted radiopharmaceuticals is promising, especially for the development of integrated diagnostic and therapeutic radiopharmaceuticals. However, it must be acknowledged that several dual-targeted combinations have fallen short of expectations in preclinical and clinical investigations. Among the prevalent challenges is the issue of target combination specificity, which

https://doi.org/10.1021/acs.jmedchem.4c01608
J. Med. Chem. 2024, 67, 21644−21670

can hinder precise quantification of the targeted lesions. Additionally, pharmacokinetic characteristics pose a challenge; excessive accumulation in nontarget organs complicates the achievement of optimal TBRs, casting doubts on the safety and efficacy of diagnostic and therapeutic interventions. Improving the sensitivity of radiotracers and reducing uptake in nontarget organs are ongoing goals of heterologous dual-targeted radiopharmaceuticals. Looking ahead, in the development of future heterologous dual-targeted radiopharmaceuticals, it is particularly important to balance the relationships among the combinations of targets, the optimization of linkers, and the selection of radionuclides. It is necessary to combine traditional radiopharmaceutical chemistry with drug design theory, especially to fully utilize the efficient and practical tools such as CADD, artificial intelligence-assisted drug design and big data models to achieve the rationality of target combination and molecule structure design in to review multiple dimensions to minimize blindness in drug development. It can be predicted that more heterologous dual-targeted radiopharmaceuticals will be developed for use in clinical diagnosis and treatment in the future.

AUTHOR INFORMATION

Corresponding Author

Junbo Zhang − *Key Laboratory of Radiopharmaceuticals of the Ministry of Education, NMPA Key Laboratory for Research and Evaluation of Radiopharmaceuticals (National Medical Products Administration), College of Chemistry, Beijing Normal University, Beijing 100875, P. R. China;* orcid.org/0000-0003-3549-6483; Email: zhjunbo@bnu.edu.cn

Authors

Zuojie Li − *Key Laboratory of Radiopharmaceuticals of the Ministry of Education, NMPA Key Laboratory for Research and Evaluation of Radiopharmaceuticals (National Medical Products Administration), College of Chemistry, Beijing Normal University, Beijing 100875, P. R. China*

Qing Ruan − *Key Laboratory of Radiopharmaceuticals of the Ministry of Education, NMPA Key Laboratory for Research and Evaluation of Radiopharmaceuticals (National Medical Products Administration), College of Chemistry and Key Laboratory of Beam Technology of the Ministry of Education, College of Physics and Astronomy, Beijing Normal University, Beijing 100875, P. R. China;* orcid.org/0000-0003-1586-1682

Yuhao Jiang − *Key Laboratory of Radiopharmaceuticals of the Ministry of Education, NMPA Key Laboratory for Research and Evaluation of Radiopharmaceuticals (National Medical Products Administration), College of Chemistry and Key Laboratory of Beam Technology of the Ministry of Education, College of Physics and Astronomy, Beijing Normal University, Beijing 100875, P. R. China;* orcid.org/0009-0004-9436-7109

Qianna Wang − *Key Laboratory of Radiopharmaceuticals of the Ministry of Education, NMPA Key Laboratory for Research and Evaluation of Radiopharmaceuticals (National Medical Products Administration), College of Chemistry, Beijing Normal University, Beijing 100875, P. R. China*

Guangxing Yin − *Key Laboratory of Radiopharmaceuticals of the Ministry of Education, NMPA Key Laboratory for Research and Evaluation of Radiopharmaceuticals (National Medical Products Administration), College of Chemistry, Beijing Normal University, Beijing 100875, P. R. China*

Junhong Feng − *Key Laboratory of Radiopharmaceuticals of the Ministry of Education, NMPA Key Laboratory for Research and Evaluation of Radiopharmaceuticals (National Medical Products Administration), College of Chemistry, Beijing Normal University, Beijing 100875, P. R. China*

Complete contact information is available at: https://pubs.acs.org/10.1021/acs.jmedchem.4c01608

Notes

The authors declare no competing financial interest.

Biographies

Zuojie Li is a Ph.D. student at the Key Laboratory of Radiopharmaceuticals of the Ministry of Education, College of Chemistry, Beijing Normal University. He obtained a Master's degree in Biochemistry and Molecular Biology from Liaocheng University. During his research, he was engaged in the design, synthesis, and antitumor mechanisms of antitumor drugs in the field of medicinal chemistry. Later, his interest shifted to the study of tumor radiopharmaceuticals. In his Ph.D, he mainly studied radiopharmaceuticals related to PSMA targets.

Qing Ruan is a postdoctor at the Key Laboratory of Radiopharmaceuticals of the Ministry of Education, and Key Laboratory of Beam Technology of the Ministry of Education, Beijing Normal University. She obtained a doctoral degree in Medicinal Chemistry and Molecular Engineering from this university. During her research, she mainly studied radiopharmaceuticals related to FAP targets.

Yuhao Jiang is a postdoctor at the Key Laboratory of Radiopharmaceuticals of the Ministry of Education, and Key Laboratory of Beam Technology of the Ministry of Education, Beijing Normal University. He obtained a doctoral degree in Medicinal Chemistry and Molecular Engineering from this university. During his research, he mainly studied radiopharmaceuticals related to antibacterial targets.

Qianna Wang is a Ph.D. student at the Key Laboratory of Radiopharmaceuticals of the Ministry of Education, College of Chemistry, Beijing Normal University. She obtained a Master's degree in Radiopharmaceutical Chemistry from this university. During her research, she mainly studied radiopharmaceuticals related to PARP targets.

Guangxing Yin is a Ph.D. student at the Key Laboratory of Radiopharmaceuticals of the Ministry of Education, College of Chemistry, Beijing Normal University. She obtained a Master's degree in Radiopharmaceutical Chemistry from this university. During her research, she mainly studied radiopharmaceuticals related to GLUTs targets.

Junhong Feng is a Ph.D. student at the Key Laboratory of Radiopharmaceuticals of the Ministry of Education, College of Chemistry, Beijing Normal University. She obtained a Master's degree in Radiopharmaceutical Chemistry from this university. During her research, she mainly studied radiopharmaceuticals related to FR targets.

Junbo Zhang is a professor at the Key Laboratory of Radiopharmaceuticals of the Ministry of Education, College of Chemistry, Beijing Normal University. He has been engaged in the research of radiopharmaceuticals for tumor and antibacterial targets, as well as the translation of these technologies into clinical settings.

ACKNOWLEDGMENTS

This work was financially supported, in part, by the National Natural Science Foundation of China (22076013, 22276015),

the Beijing Natural Science Foundation (2232010), and the Beijing Nova Program (20230484470).

■ ABBREVIATIONS

ADME, absorption, distribution, metabolism, and excretion; ALB, albumin; Aβ, amyloid β-protein; BBN, bombesin; BR, biotin receptors; CADD, computer-aided drug design; CA-IX, carbonic anhydrase 9; CTLA-4, cytotoxic T lymphocyte-associated protein 4; CXCR4, chemokine (C-X-C motif) receptor 4; DOTA, 1,4,7,10-tetraazacyclododecane-*N,N′,N,N′*-tetraacetic acid; EB, evans blue; EuK, Glu-urea-Lys; FAP, fibroblast activating protein; FDG, fludeoxyglucose; FDA, food and drug administration; GLUTs, glucose transporters; GRPR, gastrin-releasing peptide receptor; HBED-CC, *N,N′*-Bis-[2-hydroxy-5-(carboxyethyl)benzyl]ethylenediamine-*N,N′*-diacetic acid; IPBA, 4-(4-iodophenyl) butyric acid; MC1R, melanocortin-1 receptor; mCRPC, metastatic castration resistant prostate cancer; MD, molecular docking; MDS, molecular dynamics simulation; MMAE, monomethyl auristatin E; mRAIR-TC, metastatic radioiodine-refractory thyroid cancer; MTG, mitochondrial targeting groups; NETs, neuroendocrine tumors; NGR, Asp-Gly-Arg; PET, positron emission tomography; NOTA, 1,4,7-triazacyclononane-*N,N′,N″*-triaceticacid; PDC, peptide−drug conjugate; PD-1, programmed cell death inhibitor 1; PD-L1, programmed apoptosis ligand 1; PEG, polyethylene glycol; PSA, prostate specific antigen; PSMA, prostate-specific membrane antigen; RGD, Arg-Gly-Asp; RLT, radioligand therapeutic; SAR, structure−activity relationships; SPECT, single-photon emission computed tomography; SSTR, somatostatin receptor; TBRs, tumor-to-background ratios; TI, treatment index; TPP, triphenylphosphonium; Trop-2, trophoblast cell surface antigen-2; $\alpha_v\beta_6$-BP, $\alpha_v\beta_6$-binding peptide.

■ REFERENCES

(1) Rong, J.; Haider, A.; Jeppesen, T. E.; Josephson, L.; Liang, S. H. Radiochemistry for positron emission tomography. *Nat. Commun.* **2023**, *14* (1), 3257−3279.
(2) Yang, W.; Kang, F.; Chen, Y.; Zhu, Z.; Wang, F.; Qin, C.; Du, J.; Lan, X.; Wang, J. Landscape of nuclear medicine in china and its progress on theranostics. *J. Nucl. Med.* **2024**, *65* (Supplement 1), 29S−37S.
(3) Aboagye, E. O.; Barwick, T. D.; Haberkorn, U. Radiotheranostics in oncology: Making precision medicine possible. *Ca-Cancer J. Clin* **2023**, *73* (3), 255−274.
(4) Ahmed, N.; Zia, M. Diagnostic modalities and radiopharmaceuticals with particular importance of technetium-99m (^{99m}Tc). *Chin J. Acad. Radiol* **2023**, *6* (4), 143−159.
(5) Crisan, G.; Moldovean-Cioroianu, N. S.; Timaru, D. G.; Andries, G.; Cainap, C.; Chis, V. Radiopharmaceuticals for PET and SPECT imaging: A literature review over the last decade. *Int. J. Mol. Sci.* **2022**, *23* (9), 5023−5074.
(6) Wu, Y.; Sun, T.; Ng, Y. L.; Liu, J.; Zhu, X.; Cheng, Z.; Xu, B.; Meng, N.; Zhou, Y.; Wang, M. Clinical implementation of total-body PET in china. *J. Nucl. Med.* **2024**, *65* (Supplement 1), 64S−71S.
(7) Chen, W.; Li, Y.; Li, Z.; Jiang, Y.; Cui, Y.; Zeng, J.; Mo, Y.; Tang, S.; Li, S.; Liu, L.; et al. Advantages and challenges of total-body PET/CT at a tertiary cancer center: Insights from Sun Yat-sen university cancer center. *J. Nucl. Med.* **2024**, *65* (Supplement1), 54S−63S.
(8) Zhang, J. Special Issue: "Molecular Imaging in Oncology: Radiopharmaceuticals for PET and SPECT 2022. *Pharmaceuticals* **2024**, *17* (1), 49−52.
(9) Cui, X. Y.; Liu, Y.; Wang, C.; Wen, Z.; Li, Y.; Tang, H.; Diwu, J.; Yang, Y.; Cui, M.; Liu, Z. China's radiopharmaceuticals on expressway: 2014−2021. *Radiol Acta* **2022**, *110* (6−9), 765−784.
(10) Feng, H.; Wang, X.; Chen, J.; Cui, J.; Gao, T.; Gao, Y.; Zeng, W. Nuclear imaging of glucose metabolism: Beyond ^{18}F-FDG. *Contrast Media Mol. Imaging* **2019**, *2019*, 1−12.
(11) Mantel, E.; Williams, J. An introduction to newer PET diagnostic agents and related therapeutic radiopharmaceuticals. *J. Nucl. Med. Technol.* **2019**, *47* (3), 203−209.
(12) Jie, C.; Treyer, V.; Schibli, R.; Mu, L. Tauvid: The first FDA-approved PET tracer for imaging tau pathology in alzheimer's disease. *Pharmaceuticals* **2021**, *14* (2), 110.
(13) US FDA. ^{18}F-fluorodopa US approval letter [EB/OL]. October 10, 2019. https://www.accessdata.fda.gov/drugsatfda_docs/nda/2019/200655Orig1s000TOC.cfm.
(14) US FDA. Lymphoseek US approval letter [EB/OL]. March 13, 2013. https://www.accessdata.fda.gov/drugsatfda_docs/nda/2013/202207Orig1s000TOC.cfm.
(15) US FDA. Cerianna US approval letter [EB/OL]. May 20, 2020. https://www.accessdata.fda.gov/drugsatfda_docs/nda/2020/212155Orig1s000TOC.cfm.
(16) US FDA. ^{11}C-choline US approval letter [EB/OL]. September 12, 2012. https://www.accessdata.fda.gov/drugsatfda_docs/nda/2012/203155Orig1s000TOC.cfm.
(17) Farolfi, A.; Calderoni, L.; Mattana, F.; Mei, R.; Telo, S.; Fanti, S.; Castellucci, P. Current and emerging clinical applications of PSMA PET diagnostic imaging for prostate cancer. *J. Nucl. Med.* **2021**, *62* (5), 596−604.
(18) Kroenke, M.; Schweiger, L.; Horn, T.; Haller, B.; Schwamborn, K.; Wurzer, A.; Maurer, T.; Wester, H. J.; Eiber, M.; Rauscher, I. Validation of ^{18}F-rhPSMA-7 and^{18}F-rhPSMA-7.3 PET imaging results with histopathology from salvage surgery in patients with biochemical recurrence of prostate cancer. *J. Nucl. Med.* **2022**, *63* (12), 1809−1814.
(19) US FDA. Xofigo US approval letter [EB/OL]. May 15, 2013. https://www.accessdata.fda.gov/drugsatfda_docs/nda/2013/203971Orig1s000TOC.cfm.
(20) Ichikawa, Y.; Kobayashi, N.; Takano, S.; Kato, I.; Endo, K.; Inoue, T. Neuroendocrine tumor theranostics. *Cancer Sci.* **2022**, *113* (6), 1930−1938.
(21) US FDA. [^{68}Ga]Ga-DOTATOC US approval letter [EB/OL]. August 21, 2019. https://www.accessdata.fda.gov/drugsatfda_docs/nda/2019/210828Orig1s000TOC.cfm.
(22) Czernin, J.; Calais, J. ^{177}Lu-PSMA617 and the VISION trial: One of the greatest success stories in the history of nuclear medicine. *J. Nucl. Med.* **2021**, *62* (8), 1025−1026.
(23) Herrmann, K.; Schwaiger, M.; Lewis, J. S.; Solomon, S. B.; McNeil, B. J.; Baumann, M.; Gambhir, S. S.; Hricak, H.; Weissleder, R. Radiotheranostics: A roadmap for future development. *Lancet Oncol* **2020**, *21* (3), e146−e156.
(24) US FDA. Pluvicto US approval letter [EB/OL]. March 23, 2022. https://www.accessdata.fda.gov/drugsatfda_docs/nda/2022/215833Orig1s000TOC.cfm.
(25) Sgouros, G.; Bodei, L.; McDevitt, M. R.; Nedrow, J. R. Radiopharmaceutical therapy in cancer: Clinical advances and challenges. *Nat. Rev. Drug Discov* **2020**, *19* (9), 589−608.
(26) Uijen, M. J. M.; Derks, Y. H. W.; Merkx, R. I. J.; Schilham, M. G. M.; Roosen, J.; Privé, B. M.; van Lith, S. A. M.; van Herpen, C. M. L.; Gotthardt, M.; Heskamp, S.; et al. PSMA radioligand therapy for solid tumors other than prostate cancer: Background, opportunities, challenges, and first clinical reports. *Eur. J. Nucl. Med. Mol. Imaging* **2021**, *48* (13), 4350−4368.
(27) Murphy, D. G.; Sathianathen, N.; Hofman, M. S.; Azad, A.; Lawrentschuk, N. Where to next for theranostics in prostate cancer? *Eur. Urol Oncol* **2019**, *2* (2), 163−165.
(28) Sallam, M.; Nguyen, N. T.; Sainsbury, F.; Kimizuka, N.; Muyldermans, S.; Benešová-Schäfer, M. PSMA-targeted radiotheranostics in modern nuclear medicine: Then, now, and what of the future? *Theranostics* **2024**, *14* (8), 3043−3079.
(29) Elhanani, O.; Ben-Uri, R.; Keren, L. Spatial profiling technologies illuminate the tumor microenvironment. *Cancer Cell* **2023**, *41* (3), 404−420.

https://doi.org/10.1021/acs.jmedchem.4c01608
J. Med. Chem. 2024, 67, 21644−21670

(30) Sun, D. J.; Zhao, Y. Q.; Zhang, S. Y.; Zhang, L.; Liu, B.; Ouyang, L. Dual-target kinase drug design: Current strategies and future directions in cancer therapy. *Eur. J. Med. Chem.* **2020**, *188*, 112025−112039.
(31) Mu, L. M.; Ju, R. J.; Liu, R.; Bu, Y. Z.; Zhang, J. Y.; Li, X. Q.; Zeng, F.; Lu, W. L. Dual-functional drug liposomes in treatment of resistant cancers. *Adv. Drug Deliv Rev.* **2017**, *115*, 46−56.
(32) Liu, M. Y.; Ju, X. M.; Zou, J.; Shi, J. Y.; Jia, G. Q. Recent researches for dual Aurora target inhibitors in antitumor field. *Eur. J. Med. Chem.* **2020**, *203*, 112498−112512.
(33) Ye, J.; Wu, J. H.; Liu, B. Therapeutic strategies of dual-target small molecules to overcome drug resistance in cancer therapy. *BBA-Rev. Cancer* **2023**, *1878* (3), 188866−188867.
(34) Plenge, R. M.; Scolnick, E. M.; Altshuler, D. Validating therapeutic targets through human genetics. *Nat. Rev. Drug Discov* **2013**, *12* (8), 581−594.
(35) Sleep, D. Albumin and its application in drug delivery. *Expert Opin Drug Del* **2015**, *12* (5), 793−812.
(36) Lau, J.; Jacobson, O.; Niu, G.; Lin, K. S.; Bénard, F.; Chen, X. Y. Bench to bedside: Albumin binders for improved cancer radioligand therapies. *Bioconjug Chem.* **2019**, *30* (3), 487−502.
(37) Höltke, C.; Grewer, M.; Stölting, M.; Geyer, C.; Wildgruber, M.; Helfen, A. Exploring the influence of different albumin binders on molecular imaging probe distribution. *Mol. Pharmaceutics* **2021**, *18* (7), 2574−2585.
(38) Liu, Z. B.; Chen, X. Y. Simple bioconjugate chemistry serves great clinical advances: albumin as a versatile platform for diagnosis and precision therapy. *Chem. Soc. Rev.* **2016**, *45* (5), 1432−1456.
(39) Nawaz, F. Z.; Kipreos, E. T. Emerging roles for folate receptor FOLR1 in signaling and cancer. *Trends Endocrin Met* **2022**, *33* (3), 159−174.
(40) Birn, H.; Spiegelstein, O.; Christensen, E. I.; Finnell, R. H. Renal tubular reabsorption of folate mediated by folate binding protein 1. *J. Am. Soc. Nephrol* **2005**, *16* (3), 608−615.
(41) Müller, C.; Struthers, H.; Winiger, C.; Zhernosekov, K.; Schibli, R. DOTA conjugate with an albumin-binding entity enables the first folic acid-targeted ^{177}Lu-radionuclide tumor therapy in mice. *J. Nucl. Med.* **2013**, *54* (1), 124−131.
(42) Siwowska, K.; Haller, S.; Bortoli, F.; Benesová, M.; Groehn, V.; Bernhardt, P.; Schibli, R.; Müller, C. Preclinical comparison of albumin-binding radiofolates: Impact of linker entities on the *in vitro* and *in vivo* properties. *Mol. Pharmaceutics* **2017**, *14* (2), 523−532.
(43) Smit Duijzentkunst, D. A.; Kwekkeboom, D. J.; Bodei, L. Somatostatin receptor 2−targeting compounds. *J. Nucl. Med.* **2017**, *58* (Supplement 2), 54S−60S.
(44) Strosberg, J.; El-Haddad, G.; Wolin, E.; Hendifar, A.; Yao, J.; Chasen, B.; Mittra, E.; Kunz, P. L.; Kulke, M. H.; Jacene, H.; et al. Phase 3 trial of ^{177}Lu-Dotatate for midgut neuroendocrine tumors. *N Engl J. Med.* **2017**, *376* (2), 125−135.
(45) Zaknun, J. J.; Bodei, L.; Mueller-Brand, J.; Pavel, M. E.; Baum, R. P.; Hörsch, D.; O'Dorisio, M. S.; O'Dorisiol, T. M.; Howe, J. R.; Cremonesi, M.; et al. The joint IAEA, EANM, and SNMMI practical guidance on peptide receptor radionuclide therapy (PRRNT) in neuroendocrine tumours. *Eur. J. Nucl. Med. Mol. Imaging* **2013**, *40* (5), 800−816.
(46) Tian, R.; Jacobson, O.; Niu, G.; Kiesewetter, D. O.; Wang, Z.; Zhu, G.; Ma, Y.; Liu, G.; Chen, X. Evans blue attachment enhances somatostatin receptor subtype-2 imaging and radiotherapy. *Theranostics* **2018**, *8* (3), 735−745.
(47) Bandara, N.; Jacobson, O.; Mpoy, C.; Chen, X. Y.; Rogers, B. E. Novel structural modification based on evans blue dye to improve pharmacokinetics of a somastostatin-receptor-based theranostic agent. *Bioconjug Chem.* **2018**, *29* (7), 2448−2454.
(48) Zhang, J.; Wang, H.; Jacobson, O.; Cheng, Y.; Niu, G.; Li, F.; Bai, C.; Zhu, Z.; Chen, X. Safety, pharmacokinetics, and dosimetry of a long-acting radiolabeled somatostatin analog ^{177}Lu-DOTA-EB-TATE in patients with advanced metastatic neuroendocrine tumors. *J. Nucl. Med.* **2018**, *59* (11), 1699−1705.
(49) Wang, H.; Cheng, Y.; Zhang, J.; Zang, J.; Li, H.; Liu, Q.; Wang, J.; Jacobson, O.; Li, F.; Zhu, Z.; et al. Response to single low-dose ^{177}Lu-DOTA-EB-TATE treatment in patients with advanced neuroendocrine neoplasm: A prospective pilot study. *Theranostics* **2018**, *8* (12), 3308−3316.
(50) Liu, Q.; Zang, J.; Sui, H.; Ren, J.; Guo, H.; Wang, H.; Wang, R.; Jacobson, O.; Zhang, J.; Cheng, Y.; et al. Peptide receptor radionuclide therapy of late-stage neuroendocrine tumor patients with multiple cycles of ^{177}Lu-DOTA-EB-TATE. *J. Nucl. Med.* **2021**, *62* (3), 386−392.
(51) Rousseau, E.; Lau, J.; Zhang, Z.; Uribe, C. F.; Kuo, H. T.; Zhang, C.; Zeisler, J.; Colpo, N.; Lin, K. S.; Bénard, F. Effects of adding an albumin binder chain on [^{177}Lu]Lu-DOTATATE. *Nucl. Med. Biol.* **2018**, *66*, 10−17.
(52) Neels, O. C.; Kopka, K.; Liolios, C.; Afshar-Oromieh, A. Radiolabeled PSMA Inhibitors. *Cancers* **2021**, *13* (24), 6255−6278.
(53) Cornford, P.; van den Bergh, R. C. N.; Briers, E.; Van den Broeck, T.; Cumberbatch, M. G.; De Santis, M.; Fanti, S.; Fossati, N.; Gandaglia, G.; Gillessen, S.; et al. EAU-EANM-ESTRO-ESUR-SIOG guidelines on prostate cancer. part II-2020 update: Treatment of relapsing and metastatic prostate cancer. *Eur. Urol* **2021**, *79* (2), 263−282.
(54) Fanti, S.; Minozzi, S.; Antoch, G.; Banks, I.; Briganti, A.; Carrio, I.; Chiti, A.; Clarke, N.; Eiber, M.; De Bono, J.; et al. Consensus on molecular imaging and theranostics in prostate cancer. *Lancet Oncol* **2018**, *19* (12), e696−e708.
(55) Zechmann, C. M.; Afshar-Oromieh, A.; Armor, T.; Stubbs, J. B.; Mier, W.; Hadaschik, B.; Joyal, J.; Kopka, K.; Debus, J.; Babich, J. W.; et al. Radiation dosimetry and first therapy results with a ^{124}I/^{131}I I-labeled small molecule (MIP-1095) targeting PSMA for prostate cancer therapy. *Eur. J. Nucl. Med. Mol. Imaging* **2014**, *41* (7), 1280−1292.
(56) Kelly, J. M.; Amor-Coarasa, A.; Nikolopoulou, A.; Wüstemann, T.; Barelli, P.; Kim, D.; Williams, C.; Zheng, X. W.; Bi, C.; Hu, B.; et al. Dual-target binding ligands with modulated pharmacokinetics for endoradiotherapy of prostate cancer. *J. Nucl. Med.* **2017**, *58* (9), 1442−1449.
(57) Choy, C. J.; Ling, X.; Geruntho, J. J.; Beyer, S. K.; Latoche, J. D.; Langton-Webster, B.; Anderson, C. J.; Berkman, C. E. ^{177}Lu-labeled phosphoramidate-based PSMA inhibitors: The effect of an albumin binder on biodistribution and therapeutic efficacy in prostate tumor-bearing mice. *Theranostics* **2017**, *7* (7), 1928−1939.
(58) Kelly, J.; Amor-Coarasa, A.; Ponnala, S.; Nikolopoulou, A.; Williams, C.; Schlyer, D.; Zhao, Y. Z.; Kim, D.; Babich, J. W. Trifunctional PSMA-targeting constructs for prostate cancer with unprecedented localization to LNCaP tumors. *Eur. J. Nucl. Med. Mol. Imaging* **2018**, *45* (11), 1841−1851.
(59) Benesová, M.; Umbricht, C. A.; Schibli, R.; Müller, C. Albumin-binding PSMA ligands: Optimization of the tissue distribution profile. *Mol. Pharmaceutics* **2018**, *15* (3), 934−946.
(60) Kramer, V.; Fernández, R.; Lehnert, W.; Jiménez-Franco, L. D.; Soza-Ried, C.; Eppard, E.; Ceballos, M.; Meckel, M.; Benešová, M.; Umbricht, C. A.; et al. Biodistribution and dosimetry of a single dose of albumin-binding ligand [^{177}Lu]Lu-PSMA-ALB-56 in patients with mCRPC. *Eur. J. Nucl. Med. Mol. Imaging* **2021**, *48* (3), 893−903.
(61) Umbricht, C. A.; Benesová, M.; Schibli, R.; Müller, C. Preclinical development of novel PSMA-targeting radioligands: Modulation of albumin-binding properties to improve prostate cancer therapy. *Mol. Pharmaceutics* **2018**, *15* (6), 2297−2306.
(62) Kuo, H. T.; Merkens, H.; Zhang, Z.; Uribe, C. F.; Lau, J.; Zhang, C.; Colpo, N.; Lin, K. S.; Bénard, F. Enhancing treatment efficacy of ^{177}Lu-PSMA-617 with the conjugation of an albumin-binding motif: Preclinical dosimetry and endoradiotherapy studies. *Mol. Pharmaceutics* **2018**, *15* (11), 5183−5191.
(63) Wang, Z.; Jacobson, O.; Tian, R.; Mease, R. C.; Kiesewetter, D. O.; Niu, G.; Pomper, M. G.; Chen, X. Radioligand therapy of prostate cancer with a long-lasting prostate-specific membrane antigen targeting agent ^{90}Y-DOTA-EB-MCG. *Bioconjug Chem.* **2018**, *29* (7), 2309−2315.
(64) Seifert, R.; Seitzer, K.; Herrmann, K.; Kessel, K.; Schäfers, M.; Kleesiek, J.; Weckesser, M.; Boegemann, M.; Rahbar, K. Analysis of

PSMA expression and outcome in patients with advanced prostate cancer receiving ^{177}Lu-PSMA-617 radioligand therapy. *Theranostics* **2020**, *10* (17), 7812−7820.
(65) Wang, Z.; Tian, R.; Niu, G.; Ma, Y.; Lang, L.; Szajek, L. P.; Kiesewetter, D. O.; Jacobson, O.; Chen, X. Single low-dose injection of evans blue modified PSMA-617 radioligand therapy eliminates prostate-specific membrane antigen positive tumors. *Bioconjug Chem.* **2018**, *29* (9), 3213−3221.
(66) O'Keefe, D. S.; Bacich, D. J.; Huang, S. S.; Heston, W. D. W. A perspective on the evolving story of PSMA biology, PSMA-based imaging, and endoradiotherapeutic strategies. *J. Nucl. Med.* **2018**, *59* (7), 1007−1013.
(67) Wen, X.; Xu, P.; Zeng, X.; Liu, J.; Du, C.; Zeng, X.; Cheng, X.; Wang, X.; Liang, Y.; Zhao, T.; et al. Development of [^{177}Lu]Lu-LNC1003 for radioligand therapy of prostate cancer with a moderate level of PSMA expression. *Eur. J. Nucl. Med. Mol. Imaging* **2023**, *50* (9), 2846−2860.
(68) Kratochwil, C.; Bruchertseifer, F.; Giesel, F. L.; Weis, M.; Verburg, F. A.; Mottaghy, F.; Kopka, K.; Apostolidis, C.; Haberkorn, U.; Morgenstern, A. ^{225}Ac-PSMA-617 for PSMA-targeted α-radiation therapy of metastatic castration-resistant prostate cancer. *J. Nucl. Med.* **2016**, *57* (12), 1941−1944.
(69) Sathekge, M.; Bruchertseifer, F.; Knoesen, O.; Reyneke, F.; Lawal, I.; Lengana, T.; Davis, C.; Mahapane, J.; Corbett, C.; Vorster, M.; et al. ^{225}Ac-PSMA-617 in chemotherapy-naive patients with advanced prostate cancer: A pilot study. *Eur. J. Nucl. Med. Mol. Imaging* **2019**, *46* (1), 129−138.
(70) Thiele, N. A.; Brown, V.; Kelly, J. M.; Amor-Coarasa, A.; Jermilova, U.; MacMillan, S. N.; Nikolopoulou, A.; Ponnala, S.; Ramogida, C. F.; Robertson, A. K. H.; et al. An eighteen-membered macrocyclic ligand for Actinium-225 targeted alpha therapy. *Angew. Chem. Int. Edit* **2017**, *56* (46), 14712−14717.
(71) Kelly, J. M.; Amor-Coarasa, A.; Ponnala, S.; Nikolopoulou, A.; Williams, C.; Thiele, N. A.; Schlyer, D.; Wilson, J. J.; DiMagno, S. G.; Babich, J. W. A single dose of ^{225}Ac-RPS-074 induces a complete tumor response in an LNCaP xenograft model. *J. Nucl. Med.* **2019**, *60* (5), 649−655.
(72) Iikuni, S.; Tarumizu, Y.; Nakashima, K.; Higaki, Y.; Ichikawa, H.; Watanabe, H.; Ono, M. Radiotheranostics using a novel ^{225}Ac-labeled radioligand with improved pharmacokinetics targeting prostate-specific membrane antigen. *J. Med. Chem.* **2021**, *64* (18), 13429−13438.
(73) Morgenstern, A.; Apostolidis, C.; Bruchertseifer, F. Supply and clinical application of Actinium-225 and Bismuth-213. *Semin Nucl. Med.* **2020**, *50* (2), 119−123.
(74) Tsuchihashi, S.; Nakashima, K.; Tarumizu, Y.; Ichikawa, H.; Jinda, H.; Watanabe, H.; Ono, M. Development of novel ^{111}In/^{225}Ac-labeled agent targeting PSMA for highly efficient cancer radiotheranostics. *J. Med. Chem.* **2023**, *66* (12), 8043−8053.
(75) Bu, L.; Baba, H.; Yoshida, N.; Miyake, K.; Yasuda, T.; Uchihara, T.; Tan, P.; Ishimoto, T. Biological heterogeneity and versatility of cancer-associated fibroblasts in the tumor microenvironment. *Oncogene* **2019**, *38* (25), 4887−4901.
(76) Jansen, K.; Heirbaut, L.; Verkerk, R.; Cheng, J. D.; Joossens, J.; Cos, P.; Maes, L.; Lambeir, A.-M.; De Meester, I.; Augustyns, K.; et al. Extended structure−activity relationship and pharmacokinetic investigation of (4-Quinolinoyl)glycyl-2-cyanopyrrolidine inhibitors of fibroblast activation protein (FAP). *J. Med. Chem.* **2014**, *57* (7), 3053−3074.
(77) Zhao, L.; Kang, F.; Pang, Y.; Fang, J.; Sun, L.; Wu, H.; Lan, X.; Wang, J.; Chen, H. Fibroblast activation protein inhibitor tracers and their preclinical, translational, and clinical status in china. *J. Nucl. Med.* **2024**, *65* (Supplement 1), 4S−11S.
(78) Privé, B. M.; Boussihmad, M. A.; Timmermans, B.; van Gemert, W. A.; Peters, S. M. B.; Derks, Y. H. W.; van Lith, S. A. M.; Mehra, N.; Nagarajah, J.; Heskamp, S.; et al. Fibroblast activation protein-targeted radionuclide therapy: Background, opportunities, and challenges of first (pre) clinical studies. *Eur. J. Nucl. Med. Mol. Imaging* **2023**, *50* (7), 1906−1918.
(79) Ding, J.; Xu, M. X.; Chen, J. Y.; Zhang, P.; Huo, L.; Kong, Z. R.; Liu, Z. B. ^{86}Y-labeled albumin-binding fibroblast activation protein inhibitor for late-time-point cancer diagnosis. *Mol. Pharmaceutics* **2022**, *19* (9), 3429−3438.
(80) Xu, M. X.; Zhang, P.; Ding, J.; Chen, J. Y.; Huo, L.; Liu, Z. B. Albumin binder-conjugated fibroblast activation protein inhibitor radiopharmaceuticals for cancer therapy. *J. Nucl. Med.* **2022**, *63* (6), 952−958.
(81) Meng, L. X.; Fang, J. Y.; Zhao, L.; Wang, T. T.; Yuan, P.; Zhao, Z. Q.; Zhuang, R. Q.; Lin, Q.; Chen, H. J.; Chen, X. Y.; et al. Rational design and pharmacomodulation of protein-binding theranostic radioligands for targeting the fibroblast activation protein. *J. Med. Chem.* **2022**, *65* (12), 8245−8257.
(82) Mori, Y.; Dendl, K.; Cardinale, J.; Kratochwil, C.; Giesel, F. L.; Haberkorn, U. FAPI PET: Fibroblast activation protein inhibitor use in oncologic and nononcologic disease. *Radiology* **2023**, *306* (2), 220749−220763.
(83) Wen, X. J.; Xu, P. F.; Shi, M. Q.; Liu, J.; Zeng, X. Y.; Zhang, Y. R.; Shi, C. R.; Li, J. C.; Guo, Z. D.; Zhang, X. Z.; et al. Evans blue-modified radiolabeled fibroblast activation protein inhibitor as long-acting cancer therapeutics. *Theranostics* **2022**, *12* (1), 422−433.
(84) Fu, H.; Huang, J.; Zhao, T.; Wang, H.; Chen, Y.; Xu, W.; Pang, Y.; Guo, W.; Sun, L.; Wu, H.; et al. Fibroblast activation protein-targeted radioligand therapy with ^{177}Lu-EB-FAPI for metastatic radioiodine-refractory thyroid cancer: First-in-human, dose-escalation study. *Clin. Cancer Res.* **2023**, *29* (23), 4740−4750.
(85) Lin, J. J.; Chuang, C. P.; Lin, J. Y.; Huang, F. T.; Huang, C. W. Rational design, pharmacomodulation, and synthesis of [^{68}Ga]Ga-Alb-FAPtp-01, a selective tumor-associated fibroblast activation protein tracer for PET imaging of glioma. *ACS Sens* **2021**, *6* (9), 3424−3435.
(86) Millul, J.; Koepke, L.; Haridas, G. R.; Sparrer, K. M. J.; Mansi, R.; Fani, M. Head-to-head comparison of different classes of FAP radioligands designed to increase tumor residence time: Monomer, dimer, albumin binders, and small molecules vs peptides. *Eur. J. Nucl. Med. Mol. Imaging* **2023**, *50* (10), 3050−3061.
(87) Supuran, C. T. Carbonic anhydrases: Novel therapeutic applications for inhibitors and activators. *Nat. Rev. Drug Discov* **2008**, *7* (2), 168−181.
(88) Lau, J.; Lin, K. S.; Bénard, F. Past, present, and future: Development of theranostic agents targeting carbonic anhydrase IX. *Theranostics* **2017**, *7* (17), 4322−4339.
(89) Krall, N.; Pretto, F.; Mattarella, M.; Müller, C.; Neri, D. A ^{99m}Tc-labeled ligand of carbonic anhydrase IX selectively targets renal cell carcinoma *in vivo*. *J. Nucl. Med.* **2016**, *57* (6), 943−949.
(90) Iikuni, S.; Okada, Y.; Shimizu, Y.; Watanabe, H.; Ono, M. Modulation of the pharmacokinetics of a radioligand targeting carbonic anhydrase-IX with albumin-binding moieties. *Mol. Pharmaceutics* **2021**, *18* (3), 966−975.
(91) Cooper, J.; Giancotti, F. G. Integrin signaling in cancer: Mechanotransduction, stemness, epithelial plasticity, and therapeutic resistance. *Cancer Cell* **2019**, *35* (3), 347−367.
(92) Li, M.; Wang, Y.; Li, M. W.; Wu, X. Z.; Setrerrahmane, S.; Xu, H. M. Integrins as attractive targets for cancer therapeutics. *Acta Pharm. Sin B* **2021**, *11* (9), 2726−2737.
(93) Niu, G.; Chen, X. Y. Why integrin as a primary target for imaging and therapy. *Theranostics* **2011**, *1*, 30−47.
(94) Yan, Q.; Zhong, J.; Liu, Y.; Peng, S.; Feng, P.; Zhong, Y.; Hu, K. Synthesis and preclinical evaluation of a heterodimeric radioligand targeting fibroblast activation protein and integrin-$\alpha_v\beta_3$. *Eur. J. Med. Chem.* **2023**, *251*, 115279.
(95) Zang, J.; Wen, X.; Lin, R.; Zeng, X.; Wang, C.; Shi, M.; Zeng, X.; Zhang, J.; Wu, X.; Zhang, X.; et al. Synthesis, preclinical evaluation and radiation dosimetry of a dual targeting PET tracer [^{68}Ga]Ga-FAPI-RGD. *Theranostics* **2022**, *12* (16), 7180−7190.
(96) Liu, B.; Zhang, Z.; Wang, H.; Yao, S. Preclinical evaluation of a dual SSTR2 and integrin $\alpha_v\beta_3$-targeted heterodimer [^{68}Ga]-NOTA-3PEG$_4$-TATE-RGD. *Bioorg. Med. Chem.* **2019**, *27* (21), 115094−115101.

https://doi.org/10.1021/acs.jmedchem.4c01608
J. Med. Chem. 2024, 67, 21644−21670

(97) Shallal, H. M.; Minn, I.; Banerjee, S. R.; Lisok, A.; Mease, R. C.; Pomper, M. G. Heterobivalent agents targeting PSMA and integrin-$\alpha_v\beta_3$. *Bioconjug Chem.* **2014**, *25* (2), 393−405.
(98) Chen, H.; Jacobson, O.; Niu, G.; Weiss, I. D.; Kiesewetter, D. O.; Liu, Y.; Ma, Y.; Wu, H.; Chen, X. Novel "Add-On" molecule based on evans blue confers superior pharmacokinetics and transforms drugs to theranostic agents. *J. Nucl. Med.* **2017**, *58* (4), 590−597.
(99) Chen, Z. F. A neuropeptide code for itch. *Nat. Rev. Neurosci* **2021**, *22* (12), 758−776.
(100) Nock, B. A.; Kanellopoulos, P.; Joosten, L.; Mansi, R.; Maina, T. Peptide radioligands in cancer theranostics: Agonists and antagonists. *Pharmaceuticals* **2023**, *16* (5), 674−706.
(101) Stott Reynolds, T. J.; Smith, C. J.; Lewis, M. R. Peptide-based radiopharmaceuticals for molecular imaging of prostate cancer. *Adv. Exp. Med. Biol.* **2018**, *1096*, 135−158.
(102) Li, Z. B.; Wu, Z. H.; Chen, K.; Ryu, E. K.; Chen, X. Y. ^{18}F-labeled BBN-RGD heterodimer for prostate cancer imaging. *J. Nucl. Med.* **2008**, *49* (3), 453−461.
(103) Jackson, A. B.; Nanda, P. K.; Rold, T. L.; Sieckman, G. L.; Szczodroski, A. F.; Hoffman, T. J.; Chen, X. Y.; Smith, C. J. ^{64}Cu-NO2A-RGD-Glu-6-Ahx-BBN(7−14)NH_2: A heterodimeric targeting vector for positron emission tomography imaging of prostate cancer. *Nucl. Med. Biol.* **2012**, *39* (3), 377−387.
(104) Liu, Z. F.; Niu, G.; Wang, F.; Chen, X. Y. ^{68}Ga-labeled NOTA-RGD-BBN peptide for dual integrin and GRPR-targeted tumor imaging. *Eur. J. Nucl. Med. Mol. Imaging* **2009**, *36* (9), 1483−1494.
(105) Liu, Z. F.; Huang, J. M.; Dong, C. Y.; Cui, L. Y.; Jin, X. N.; Jia, B.; Zhu, Z. H.; Li, F.; Wang, F. ^{99m}Tc-labeled RGD-BBN peptide for small-animal SPECT/CT of lung carcinoma. *Mol. Pharmaceutics* **2012**, *9* (5), 1409−1417.
(106) Hu, K.; Tang, X.; Tang, G.; Yao, S.; Yao, B.; Wang, H.; Nie, D.; Liang, X.; Tang, C.; He, S.; et al. ^{18}F-FP-PEG_2-β-Glu-RGD_2: A Symmetric integrin $\alpha_v\beta_3$-targeting radiotracer for tumor PET imaging. *PLoS One* **2015**, *10* (9), 138675−138688.
(107) Durkan, K.; Jiang, Z.; Rold, T. L.; Sieckman, G. L.; Hoffman, T. J.; Bandari, R. P.; Szczodroski, A. F.; Liu, L.; Miao, Y.; Reynolds, T. S.; et al. A heterodimeric [RGD-Glu-[^{64}Cu-NO2A]-6-Ahx-RM2] $\alpha_v\beta_3$/GRPr-targeting antagonist radiotracer for PET imaging of prostate tumors. *Nucl. Med. Biol.* **2014**, *41* (2), 133−139.
(108) Zhang, J.; Niu, G.; Lang, L.; Li, F.; Fan, X.; Yan, X.; Yao, S.; Yan, W.; Huo, L.; Chen, L.; et al. Clinical translation of a dual integrin $\alpha_v\beta_3$- and gastrin-releasing peptide receptor−targeting PET radiotracer, ^{68}Ga-BBN-RGD. *J. Nucl. Med.* **2017**, *58* (2), 228−234.
(109) Zhang, J.; Mao, F.; Niu, G.; Peng, L.; Lang, L.; Li, F.; Ying, H.; Wu, H.; Pan, B.; Zhu, Z.; et al. ^{68}Ga-BBN-RGD PET/CT for GRPR and integrin $\alpha_v\beta_3$ imaging in patients with breast cancer. *Theranostics* **2018**, *8* (4), 1121−1130.
(110) Wen, X.; Wang, R.; Xu, P.; Shi, M.; Shang, Q.; Zeng, X.; Zeng, X.; Liu, J.; Wang, X.; Zhu, Z.; et al. Synthesis, preclinical, and initial clinical evaluation of integrin $\alpha_V\beta_3$ and gastrin-releasing peptide receptor (GRPR) dual-targeting radiotracer [^{68}Ga]Ga-RGD-RM26−03. *Eur. J. Nucl. Med. Mol. Imaging* **2024**, *51* (7), 2023−2035.
(111) Bononi, G.; Iacopini, D.; Cicio, G.; Di Pietro, S.; Granchi, C.; Di Bussolo, V.; Minutolo, F. Glycoconjugated metal complexes as cancer diagnostic and therapeutic agents. *ChemMedChem.* **2021**, *16* (1), 30−64.
(112) Kaanders, J. H. A. M.; Bussink, J.; Aarntzen, E. H. J. G.; Braam, P.; Rütten, H.; van der Maazen, R. W. M.; Verheij, M.; van den Bosch, S. [^{18}F]FDG-PET-based personalized radiotherapy dose prescription. *Semin Radiat Oncol* **2023**, *33* (3), 287−297.
(113) Haubner, R.; Kuhnast, B.; Mang, C.; Weber, W. A.; Kessler, H.; Wester, H. J.; Schwaiger, M. [^{18}F]Galacto-RGD: Synthesis, radiolabeling, metabolic stability, and radiation dose estimates. *Bioconjug Chem.* **2004**, *15* (1), 61−69.
(114) Doss, M.; Kolb, H. C.; Zhang, J. J.; Bélanger, M. J.; Stubbs, J. B.; Stabin, M. G.; Hostetler, E. D.; Alpaugh, R. K.; von Mehren, M.; Walsh, J. C.; et al. Biodistribution and radiation dosimetry of the integrin marker ^{18}F-RGD-K5 determined from whole-body PET/CT in monkeys and humans. *J. Nucl. Med.* **2012**, *53* (5), 787−795.
(115) Bhagwat, S. V.; Lahdenranta, J.; Giordano, R.; Arap, W.; Pasqualini, R.; Shapiro, L. H. CD13/APN is activated by angiogenic signals and is essential for capillary tube formation. *Blood* **2001**, *97* (3), 652−659.
(116) Gai, Y.; Jiang, Y.; Long, Y.; Sun, L.; Liu, Q.; Qin, C.; Zhang, Y.; Zeng, D.; Lan, X. Evaluation of an integrin $\alpha_v\beta_3$ and aminopeptidase N dual-receptor targeting tracer for breast cancer imaging. *Mol. Pharmaceutics* **2020**, *17* (1), 349−358.
(117) Buck, A. K.; Serfling, S. E.; Lindner, T.; Hänscheid, H.; Schirbel, A.; Hahner, S.; Fassnacht, M.; Einsele, H.; Werner, R. A. CXCR4-targeted theranostics in oncology. *Eur. J. Nucl. Med. Mol. Imaging* **2022**, *49* (12), 4133−4144.
(118) Chatterjee, S.; Behnam Azad, B.; Nimmagadda, S. The intricate role of CXCR4 in cancer. *Adv. Cancer Res.* **2014**, *124*, 31−82.
(119) Jiang, Y.; Long, Y.; Ji, H.; Qiao, P.; Liu, Q.; Xia, X.; Qin, C.; Zhang, Y.; Lan, X.; Gai, Y. Development and evaluation of a peptide heterodimeric tracer targeting CXCR4 and integrin $\alpha_v\beta_3$ for pancreatic cancer imaging. *Pharmaceutics* **2022**, *14* (9), 1791−1806.
(120) Shi, H.; Cheng, Z. MC1R and melanin-based molecular probes for theranostic of melanoma and beyond. *Acta Pharmacol Sin* **2022**, *43* (12), 3034−3044.
(121) Böhm, M.; Robert, C.; Malhotra, S.; Clément, K.; Farooqi, S. An overview of benefits and risks of chronic melanocortin-1 receptor activation. *J. Eur. Acad. Dermatol Venereol* **2024**.
(122) Eberle, A. N.; Froidevaux, S. Radiolabeled a-melanocyte-stimulating hormone analogs for receptor-mediated targeting of melanoma: From tritium to indium. *J. Mol. Recognit* **2003**, *16* (5), 248−254.
(123) Flook, A. M.; Yang, J.; Miao, Y. Evaluation of New Tc-99m-labeled Arg-X-Asp-conjugated a-Melanocyte stimulating hormone peptides for melanoma imaging. *Mol. Pharmaceutics* **2013**, *10* (9), 3417−3424.
(124) Flook, A. M.; Yang, J.; Miao, Y. Effects of amino acids on melanoma targeting and clearance properties of Tc-99m-labeled Arg-X-Asp-conjugated a-melanocyte stimulating hormone peptides. *J. Med. Chem.* **2013**, *56* (21), 8793−8802.
(125) Flook, A. M.; Yang, J.; Miao, Y. Substitution of the Lys Linker with the B-Ala Linker Dramatically Decreased the Renal Uptake of ^{99m}Tc-labeled Arg-X-Asp-conjugated and X-Ala-Asp-conjugated a-melanocyte stimulating hormone peptides. *J. Med. Chem.* **2014**, *57* (21), 9010−9018.
(126) Yang, J.; Hu, C.-A. A.; Miao, Y. Tc-99m-labeled RGD-conjugated alpha-melanocyte stimulating hormone hybrid peptides with reduced renal uptake. *Amino Acids* **2015**, *47* (4), 813−823.
(127) Reader, C. S.; Vallath, S.; Steele, C. W.; Haider, S.; Brentnall, A.; Desai, A.; Moore, K. M.; Jamieson, N. B.; Chang, D.; Bailey, P.; et al. The integrin $\alpha_v\beta_6$ drives pancreatic cancer through diverse mechanisms and represents an effective target for therapy. *J. Pathol* **2019**, *249* (3), 332−342.
(128) Hausner, S. H.; Bold, R. J.; Cheuy, L. Y.; Chew, H. K.; Daly, M. E.; Davis, R. A.; Foster, C. C.; Kim, E. J.; Sutcliffe, J. L. Preclinical development and first-in-human imaging of the integrin $\alpha_v\beta_6$ with [^{18}F]$\alpha_v\beta_6$-binding peptide in metastatic carcinoma. *Clin. Cancer Res.* **2019**, *25* (4), 1206−1215.
(129) Alas, M.; Saghaeidehkordi, A.; Kaur, K. Peptide−drug conjugates with different linkers for cancer therapy. *J. Med. Chem.* **2021**, *64* (1), 216−232.
(130) Davis, R. A.; Ganguly, T.; Harris, R.; Hausner, S. H.; Kovacs, L.; Sutcliffe, J. L. Synthesis and evaluation of a monomethyl auristatin E-integrin $\alpha_v\beta_6$ binding peptide−drug conjugate for tumor targeted drug delivery. *J. Med. Chem.* **2023**, *66* (14), 9842−9852.
(131) Wang, P.; Wang, S. L.; Liu, F. T.; Ren, Y. N.; Guo, Q.; Zhang, Q.; Hou, X. G.; Yao, Y.; Zhu, H.; Yang, Z. Preclinical evaluation of a fibroblast activation protein and a prostate-specific membrane antigen dual-targeted probe for noninvasive prostate cancer imaging. *Mol. Pharmaceutics* **2023**, *20* (2), 1415−1425.
(132) Boinapally, S.; Lisok, A.; Lofland, G.; Minn, I.; Yan, Y.; Jiang, Z.; Shin, M. J.; Merino, V. F.; Zheng, L.; Brayton, C.; et al. Hetero-bivalent

agents targeting FAP and PSMA. *Eur. J. Nucl. Med. Mol. Imaging* **2022**, *49* (13), 4369−4381.
(133) Hu, K.; Li, L.; Huang, Y.; Ye, S.; Zhong, J.; Yan, Q.; Zhong, Y.; Fu, L.; Feng, P.; Li, H. Radiosynthesis and preclinical evaluation of bispecific PSMA/FAP heterodimers for tumor imaging. *Pharmaceuticals* **2022**, *15* (3), 383−397.
(134) Verena, A.; Zhang, Z.; Kuo, H. T.; Merkens, H.; Zeisler, J.; Wilson, R.; Bendre, S.; Wong, A. A. W. L.; Bénard, F.; Lin, K. S. Synthesis and preclinical evaluation of three novel ^{68}Ga-labeled bispecific PSMA/FAP-targeting tracers for prostate cancer imaging. *Molecules* **2023**, *28* (3), 1088−1105.
(135) Zhu, W. J.; Cheng, Y. J.; Jia, R.; Zhao, H.; Bai, C. M.; Xu, J. M.; Yao, S. B.; Huo, L. A prospective, randomized, double-blind study to evaluate the safety, biodistribution, and dosimetry of ^{68}Ga-NODAGA-LM3 and ^{68}Ga-DOTA-LM3 in patients with well-differentiated neuroendocrine tumors. *J. Nucl. Med.* **2021**, *62* (10), 1398−1405.
(136) Wild, D.; Fani, M.; Behe, M.; Brink, I.; Rivier, J. E. F.; Reubi, J. C.; Maecke, H. R.; Weber, W. A. First clinical evidence that imaging with somatostatin receptor antagonists is feasible. *J. Nucl. Med.* **2011**, *52* (9), 1412−1417.
(137) Fani, M.; Nicolas, G. P.; Wild, D. Somatostatin receptor antagonists for imaging and therapy. *J. Nucl. Med.* **2017**, *58* (Supplement2), 61s−66s.
(138) Zhao, L.; Pang, Y.; Fang, J.; Chen, J.; Zhou, Y.; Sun, L.; Wu, H.; Guo, Z.; Lin, Q.; Chen, H. Design, preclinical evaluation, and clinical translation of ^{68}Ga-FAPI-LM3, a heterobivalent molecule for PET imaging of nasopharyngeal carcinoma. *J. Nucl. Med.* **2024**, *65* (3), 394−401.
(139) Tripathi, R.; Guglani, A.; Ghorpade, R.; Wang, B. Biotin conjugates in targeted drug delivery: is it mediated by a biotin transporter, a yet to be identified receptor, or (an) other unknown mechanism (s) ? *J. Enzyme Inhib Med. Chem.* **2023**, *38* (1), 2276663−2276678.
(140) Udompholkul, P.; Baggio, C.; Gambini, L.; Sun, Y.; Zhao, M.; Hoffman, R. M.; Pellecchia, M. Effective tumor targeting by EphA2-agonist-biotin-streptavidin conjugates. *Molecules* **2021**, *26* (12), 3687−3699.
(141) Chen, X.; Xia, D.; Zeng, X.; Meng, L.; Wang, Y.; Li, H.; Zhang, J.; Zhao, Z.; Zhuang, R.; Fang, J.; et al. Rational design and pharmacomodulation of ^{18}F-labeled Biotin/FAPI-conjugated heterodimers. *J. Med. Chem.* **2024**, *67* (10), 8361−8371.
(142) Potemkin, R.; Strauch, B.; Kuwert, T.; Prante, O.; Maschauer, S. Development of ^{18}F-Fluoroglycosylated PSMA-ligands with improved renal clearance behavior. *Mol. Pharmaceutics* **2020**, *17* (3), 933−943.
(143) Aso, A.; Nabetani, H.; Matsuura, Y.; Kadonaga, Y.; Shirakami, Y.; Watabe, T.; Yoshiya, T.; Mochizuki, M.; Ooe, K.; Kawakami, A.; et al. Evaluation of Astatine-211-labeled fibroblast activation protein inhibitor (FAPI): Comparison of different linkers with polyethylene glycol and piperazine. *Int. J. Mol. Sci.* **2023**, *24* (10), 8701−8713.
(144) Toms, J.; Kogler, J.; Maschauer, S.; Daniel, C.; Schmidkonz, C.; Kuwert, T.; Prante, O. Targeting fibroblast activation protein: Radiosynthesis and preclinical evaluation of an ^{18}F-labeled FAP inhibitor. *J. Nucl. Med.* **2020**, *61* (12), 1806−1813.
(145) Bolcaen, J.; Gizawy, M. A.; Terry, S. Y. A.; Paulo, A.; Cornelissen, B.; Korde, A.; Engle, J.; Radchenko, V.; Howell, R. W. Marshalling the potential of auger electron radiopharmaceutical therapy. *J. Nucl. Med.* **2023**, *64* (9), 1344−1351.
(146) Averbeck, D.; Rodriguez-Lafrasse, C. Role of mitochondria in radiation responses: Epigenetic, metabolic, and signaling impacts. *Int. J. Mol. Sci.* **2021**, *22* (20), 11047−11105.
(147) Richardson, R. B.; Harper, M.-E. Mitochondrial stress controls the radiosensitivity of the oxygen effect: Implications for radiotherapy. *Oncotarget* **2016**, *7* (16), 21469−21483.
(148) Battogtokh, G.; Choi, Y. S.; Kang, D. S.; Park, S. J.; Shim, M. S.; Huh, K. M.; Cho, Y. Y.; Lee, J. Y.; Lee, H. S.; Kang, H. C. Mitochondria-targeting drug conjugates for cytotoxic, anti-oxidizing and sensing purposes: Current strategies and future perspectives. *Acta Pharm. Sin B* **2018**, *8* (6), 862−880.
(149) Figueiredo, D.; Fernandes, C.; Silva, F.; Palma, E.; Raposinho, P.; Belchior, A.; Vaz, P.; Paulo, A. Synthesis and biological evaluation of ^{99m}Tc (I) tricarbonyl complexes dual-targeted at tumoral mitochondria. *Molecules* **2021**, *26* (2), 441−465.
(150) Santos, J. F.; Braz, M. T.; Raposinho, P.; Cleeren, F.; Cassells, I.; Leekens, S.; Cawthorne, C.; Mendes, F.; Fernandes, C.; Paulo, A. Synthesis and preclinical evaluation of PSMA-targeted ^{111}In-radioconjugates containing a mitochondria-tropic triphenylphosphonium carrier. *Mol. Pharmaceutics* **2024**, *21* (1), 216−233.
(151) Bandari, R. P.; Jiang, Z.; Reynolds, T. S.; Bernskoetter, N. E.; Szczodroski, A. F.; Bassuner, K. J.; Kirkpatrick, D. L.; Rold, T. L.; Sieckman, G. L.; Hoffman, T. J.; et al. Synthesis and biological evaluation of copper-64 radiolabeled [DUPA-6-Ahx-(NODAGA)-5-Ava-BBN(7−14)NH_2], a novel bivalent targeting vector having affinity for two distinct biomarkers (GRPR/PSMA) of prostate cancer. *Nucl. Med. Biol.* **2014**, *41* (4), 355−363.
(152) Mendoza-Figueroa, M. J.; Escudero-Castellanos, A.; Ramirez-Nava, G. J.; Ocampo-García, B. E.; Santos-Cuevas, C. L.; Ferro-Flores, G.; Pedraza-Lopez, M.; Avila-Rodriguez, M. A. Preparation and preclinical evaluation of ^{68}Ga-iPSMA-BN as a potential heterodimeric radiotracer for PET-imaging of prostate cancer. *J. Radioanal Nucl. Chem.* **2018**, *318* (3), 2097−2105.
(153) Rivera-Bravo, B.; Ramírez-Nava, G.; Mendoza-Figueroa, M. J.; Ocampo-García, B.; Ferro-Flores, G.; Ávila-Rodríguez, M. A.; Santos-Cuevas, C. [^{68}Ga]Ga-iPSMA-Lys^3-bombesin: Biokinetics, dosimetry and first patient PET/CT imaging. *Nucl. Med. Biol.* **2021**, *96*, 54−60.
(154) Eder, M.; Schäfer, M.; Bauder-Wüst, U.; Haberkorn, U.; Eisenhut, M.; Kopka, K. Preclinical evaluation of a bispecific low-molecular heterodimer targeting both PSMA and GRPR for improved PET imaging and therapy of prostate cancer. *Prostate* **2014**, *74* (6), 659−668.
(155) Liolios, C.; Schäfer, M.; Haberkorn, U.; Eder, M.; Kopka, K. Novel bispecific PSMA/GRPR targeting radioligands with optimized pharmacokinetics for improved PET imaging of prostate cancer. *Bioconjug Chem.* **2016**, *27* (3), 737−751.
(156) Korman, A. J.; Garrett-Thomson, S. C.; Lonberg, N. The foundations of immune checkpoint blockade and the ipilimumab approval decennial. *Nat. Rev. Drug Discov* **2022**, *21* (7), 509−528.
(157) Hodi, F. S.; Chiarion-Sileni, V.; Gonzalez, R.; Grob, J. J.; Rutkowski, P.; Cowey, C. L.; Lao, C. D.; Schadendorf, D.; Wagstaff, J.; Dummer, R.; et al. Nivolumab plus ipilimumab or nivolumab alone versus ipilimumab alone in advanced melanoma (CheckMate 067): 4-year outcomes of a multicentre, randomised, phase 3 trial. *Lancet Oncol* **2018**, *19* (11), 1480−1492.
(158) Jiang, C.; Zhang, L.; Xu, X.; Qi, M.; Zhang, J.; He, S.; Tian, Q.; Song, S. Engineering a smart agent for enhanced immunotherapy effect by simultaneously blocking PD-L1 and CTLA-4. *Adv. Sci.* **2021**, *8* (20), 2102500.
(159) Jiang, C.; Tian, Q.; Xu, X.; Li, P.; He, S.; Chen, J.; Yao, B.; Zhang, J.; Yang, Z.; Song, S. Enhanced antitumor immune responses via a new agent [^{131}I]-labeled dual-target immunosuppressant. *Eur. J. Nucl. Med. Mol. Imaging* **2023**, *50* (2), 275−286.
(160) Pennington, L. D.; Hesse, M. J.; Koester, D. C.; McAtee, R. C.; Qunies, A. a. M.; Hu, D. X. Property-based drug design merits a nobel prize. *J. Med. Chem.* **2024**, *67* (14), 11452−11458.
(161) Pennington, L. D. Total synthesis as training for medicinal chemistry. *ACS Med. Chem. Lett.* **2024**, *15* (2), 156−158.
(162) Odugbemi, A. I.; Nyirenda, C.; Christoffels, A.; Egieyeh, S. A. Artificial intelligence in antidiabetic drug discovery: The advances in QSAR and the prediction of a-glucosidase inhibitors. *Comput. Struct Biotechnol J.* **2024**, *23*, 2964−2977.
(163) van De Waterbeemd, H.; Smith, D. A.; Beaumont, K.; Walker, D. K. Property-based design: Optimization of drug absorption and pharmacokinetics. *J. Med. Chem.* **2001**, *44* (9), 1313−1333.
(164) Schneider, P.; Walters, W. P.; Plowright, A. T.; Sieroka, N.; Listgarten, J.; Goodnow, R. A., Jr; Fisher, J.; Jansen, J. M.; Duca, J. S.; Rush, T. S.; Zentgraf, M.; Hill, J. E.; Krutoholow, E.; Kohler, M.; Blaney, J.; Funatsu, K.; Luebkemann, C.; Schneider, G. Rethinking drug design

https://doi.org/10.1021/acs.jmedchem.4c01608
J. Med. Chem. 2024, 67, 21644−21670

in the artificial intelligence era. *Nat. Rev. Drug Discov* **2020**, *19* (5), 353−364.
(165) Cai, J.; Lian, C.; Lu, Z.; Shang, Q.; Wang, L.; Han, Z.; Gu, Y. FGF_{19}-based mini probe targeting $FGFR_4$ for diagnosis and surgical navigation of hepatocellular carcinoma. *J. Med. Chem.* **2024**, *67* (5), 3764−3777.
(166) Gao, M.; Han, Z.; Zhou, L.; Li, P.; Xu, H.; Gu, Y.; Ma, Y. DNA framework-programmed ligand positioning to modulate the targeting performance. *ACS Appl. Mater. Interfaces* **2022**, *14* (32), 36957−36965.
(167) Zhou, L.; Yu, B.; Gao, M.; Chen, R.; Li, Z.; Gu, Y.; Bian, J.; Ma, Y. DNA framework-engineered chimeras platform enables selectively targeted protein degradation. *Nat. Commun.* **2023**, *14* (1), 4510.
(168) Fan, J.; de Lannoy, I. A. M. Pharmacokinetics. *Biochem. Pharmacol.* **2014**, *87* (1), 93−120.

https://doi.org/10.1021/acs.jmedchem.4c01608
J. Med. Chem. 2024, 67, 21644−21670